AD-A185 911 OPERATING CHARACTERISTICS FOR CLIPPING OF IN-PHASE AND 1/1
QUADRATURE COMPONE..(U) NAVAL UNDERWATER SYSTEMS CENTER
NEW LONDON CT NEW LONDON LAB.. A H NUTTALL 30 JUN 86
UNCLASSIFIED NUSC-TR-7757 F/G 9/1 NL

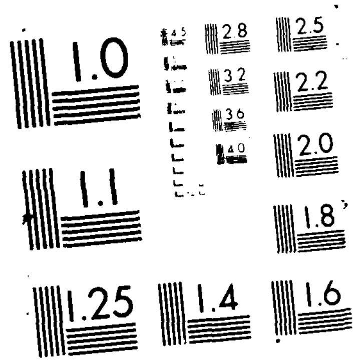
1.0
1.1
1.25
1.4
1.6
1.8
2.0
2.2
2.5
2.8
3.2
3.6
4.0

NUSC Technical Report 7757
30 June 1986

Operating Characteristics for Clipping of In-Phase and Quadrature Components of Input and/or Reference of Narrowband Correlator

Albert H. Nuttall
Suface Ship Sonar Department

Naval Underwater Systems Center

Newport, Rhode Island / New London, Connecticut

Preface

This research was conducted under NUSC Project No. J20024, "Surface Ship ASW Advanced Development," Principal Investigator Ira B. Cohen (Code 33142), Program Manager David M. Ashworth (Code 33A4), sponsored by Naval Sea Systems Command, Program Element 63553N, Subproject/Task S1704, Program Manager CDR Edward Graham IV (NAVSEA 63D). Also this research was conducted under NUSC Project No. A75205, Subproject No. ZR0000101, "Applications of Statistical Communication Theory to Acoustic Signal Processing," Principal Investigator Dr. Albert H. Nuttall (Code 3314), sponsored by the NUSC In-House Independent Research Program, Manager Mr. W. R. Hunt, Director of Navy Laboratories (SPAWAR 05).

The Technical Reviewer of this report was Ira B. Cohen (Code 33142).

Reviewed and Approved: 30 June 1986

W A Von Winkle

W. A. Von Winkle
Associate Technical Director
for Technology

UNCLASSIFIED
SECURITY CLASSIFICATION OF THIS PAGE

REPORT DOCUMENTATION PAGE

1a. REPORT SECURITY CLASSIFICATION
UNCLASSIFIED

1b. RESTRICTIVE MARKINGS

2a. SECURITY CLASSIFICATION AUTHORITY

2b. DECLASSIFICATION / DOWNGRADING SCHEDULE

3. DISTRIBUTION / AVAILABILITY OF REPORT
Approved for public release;
distribution unlimited

4. PERFORMING ORGANIZATION REPORT NUMBER(S)
TR 7757

5. MONITORING ORGANIZATION REPORT NUMBER(S)

6a. NAME OF PERFORMING ORGANIZATION
Naval Underwater Systems Center

6b. OFFICE SYMBOL *(If applicable)*

7a. NAME OF MONITORING ORGANIZATION

6c. ADDRESS *(City, State, and ZIP Code)*
New London Laboratory
New London, CT 06320

7b. ADDRESS *(City, State, and ZIP Code)*

8a. NAME OF FUNDING / SPONSORING ORGANIZATION
Naval Sea Systems Command

8b. OFFICE SYMBOL *(If applicable)*

9. PROCUREMENT INSTRUMENT IDENTIFICATION NUMBER

8c. ADDRESS *(City, State, and ZIP Code)*
Department of the Navy
Washington, DC 20362

10. SOURCE OF FUNDING NUMBERS

PROGRAM ELEMENT NO.	PROJECT NO.	TASK NO.	WORK UNIT ACCESSION NO.

11. TITLE *(Include Security Classification)*
OPERATING CHARACTERISTICS FOR CLIPPING OF IN-PHASE AND QUADRATURE COMPONENTS OF INPUT AND/OR REFERENCE OF NARROWBAND CORRELATOR

12. PERSONAL AUTHOR(S)

13a. TYPE OF REPORT

13b. TIME COVERED FROM ________ TO ________

14. DATE OF REPORT *(Year, Month, Day)*
1986 June 30

15. PAGE COUNT

16. SUPPLEMENTARY NOTATION

17. COSATI CODES

FIELD	GROUP	SUB-GROUP

18. SUBJECT TERMS *(Continue on reverse if necessary and identify by block number)*
Operating Characteristics
Quadrature Components
Clipped Input
Clipped Reference
Narrowband Correlator
Detection Probability

19. ABSTRACT *(Continue on reverse if necessary and identify by block number)*

For a narrowband waveform, the possibility of clipping both the in-phase and quadrature components of the input and reference for a cross-correlator is investigated analytically and confirmed numerically via simulation. Specifically, detection and false alarm probabilities are evaluated when the correlator input and/or the local reference are hard-clipped; in addition, these same probabilities are determined for the completely linear system. Results for typical signals reveal degradations, due to clipping, of the order of 1 to 3 dB, depending on the precise location of the clipper(s) and the particular signal waveform.

Similar results are derived and evaluated for a baseband system, where only one clipper is employed on the single channel input and/or one clipper is used for the local reference. Comparisons with the two-clipper narrowband system reveal

20. DISTRIBUTION / AVAILABILITY OF ABSTRACT
☒ UNCLASSIFIED/UNLIMITED ☐ SAME AS RPT ☐ DTIC USERS

21. ABSTRACT SECURITY CLASSIFICATION
UNCLASSIFIED

22a. NAME OF RESPONSIBLE INDIVIDUAL
Albert H. Nuttall

22b. TELEPHONE *(Include Area Code)*
(203) 440-4618

22c. OFFICE SYMBOL
Code 3314

DD FORM 1473, 84 MAR

83 APR edition may be used until exhausted
All other editions are obsolete

SECURITY CLASSIFICATION OF THIS PAGE
UNCLASSIFIED

18. SUBJECT TERMS (Cont'd.)

False Alarm Probability

19. ABSTRACT (Cont'd.)

virtually identical degradations; thus, the inclusion of the extra clipper(s) in the second (quadrature) channel of a narrowband correlator does not ameliorate the degradation, but only serves to maintain it at the same level as for the baseband system.

TABLE OF CONTENTS

Page

TABLE OF CONTENTS (Cont'd)

LIST OF ILLUSTRATIONS

LIST OF SYMBOLS

ROC	Receiver operating characteristics
K	Number of samples in accumulator
P_D	Probability of detection
P_F	Probability of false alarm
x_k	Input at time k, (1),(44)
s_k	Input signal
n_k	Input noise
H_0	Hypothesis that signal is absent
H_1	Hypothesis that signal is present
σ_n	Noise input standard deviation, (45),(47)
g	Nonlinearity, (2)
sgn(x)	+1 for x > 0, -1 for x < 0
v_k	Nonlinearity output, (3),(48)
w_k	Correlator local reference, (4),(49)
z	Accumulator output, (5),(50)
m_z	Mean of z, (6),(76)
σ_z	Standard deviation of z, (6),(85)
T	Threshold, (7),(58)
Φ	Normal probability integral, (8)
ϕ	Normal Gaussian density, (8)
d	Deflection for linear-input correlator, (9),(60)
$\tilde{\Phi}$	Inverse function to Φ, (11)
E	Received signal energy, (12),(63)

LIST OF SYMBOLS (Cont'd)

d_m	Deflection for matched reference, (12),(63)
d_r	Deflection for clipped reference, (13),(65)
a	Cosine signal amplitude, (14),(66)
overbar	Ensemble average, (21),(74)
G_p	p-th moment, (21),(74)
sub o	Signal absent, (23)
Δ	Deflection for clipped-input correlator, (25),(88)
Δ_m	Deflection for matched reference, (35),(91)
Δ_r	Deflection for clipped reference, (36),(92)
Θ	Random phase shift, (44)
sub r	Real part, (46)
sub i	Imaginary part, (46)
γ	Narrowband correlator output, (51)
S	Signal component of z, (53)
N	Noise component of z, (53)
σ_N^2	Variance of N, (54),(56)
Q	Q-function, (58)
t_k	Auxiliary variable, (72)
α_k, β_k	Auxiliary variables, (78)

Reverse Blank

OPERATING CHARACTERISTICS FOR CLIPPING OF IN-PHASE AND QUADRATURE COMPONENTS OF INPUT AND/OR REFERENCE OF NARROWBAND CORRELATOR

INTRODUCTION

To minimize the amount of data processing, telemetry bandwidth, execution time, and storage, hard clipping is frequently employed in signal processing hardware. In particular, for cross-correlation of a received input waveform with a local reference, several alternatives exist for inclusion of clipping. Either the input or the reference or both could be clipped. For a narrowband system, where the input is complex demodulated, the further option of employing clipping in both the in-phase and quadrature channels, of the input as well as reference, is available.

Here we will investigate all the various possibilities of including clipping at the input and/or reference level, for both baseband (real) and narrowband (complex) signal processing systems. In this manner, we will ascertain whether inclusion of the additional clippers in the quadrature channels ameliorates the degradation associated with the usual case of a single clipper operating on one real input process.

For completeness, we will present the analysis and simulation for both the baseband correlator as well as the narrowband correlator. This will serve as verification of the analysis technique and afford a ready comparison of both types of correlators.

No definitions of output signal-to-noise ratio criteria are employed here. Rather, we evaluate the system output detection probability P_D and false alarm probability P_F in terms of the input signal-to-noise ratio, which is a well defined quantity. We can then make a direct comparison between systems, of the required input signal-to-noise ratios, in order to achieve some specified common performance level P_D, P_F.

PROBABILITIES FOR LINEAR-INPUT CHANNEL

In this subsection, we presume that the nonlinearity g in the input channel of figure 1 is absent; that is, from (2) and (3), $v_k = x_k$. The output of the correlator is then, for signal present,

$$z = \sum_k w_k v_k = \sum_k w_k x_k = \sum_k w_k (s_k + n_k) \ , \tag{5}$$

where $\sum_k$ denotes the sum from k=1 to K. It is important to observe that signal waveform $\{s_k\}$ and reference $\{w_k\}$ are completely general at this point. That is, we have <u>not</u> restricted consideration to the examples of (4) yet.

Since process $\{n_k\}$ is Gaussian, the random variable z in (5) is also Gaussian. It has mean and variance

$$m_z = \sum_k w_k s_k \quad , \quad \sigma_z^2 = \sigma_n^2 \sum_k w_k^2 \ . \tag{6}$$

(The latter relation also holds true when the signal is absent.) The detection probability is then, for threshold T,

$$P_D = \mathrm{Prob}(z > T) = \int_T^{\infty} \frac{du}{(2\pi)^{1/2}\sigma_z} \exp\left[-\frac{(u - m_z)^2}{2\sigma_z^2}\right] = \Phi\left(d - \frac{T}{\sigma_z}\right) , \tag{7}$$

where normal probability integral

$$\Phi(x) = \int_{-\infty}^{x} dt\ (2\pi)^{-1/2} \exp\left(-t^2/2\right) \equiv \int_{-\infty}^{x} dt\ \phi(t) \tag{8}$$

and deflection parameter

$$d \equiv \frac{m_z}{\sigma_z} = \frac{\sum_k w_k s_k}{\sigma_n \left(\sum_k w_k^2\right)^{1/2}} . \tag{9}$$

The false alarm probability is obtained by setting the signal $\{s_k\}$ equal to zero in (9) and (7):

$$P_F = \Phi(-T/\sigma_z) . \tag{10}$$

Combining (7) and (10), we have the exact performance (receiver operating) characteristics in the compact form

$$P_D = \Phi\left(d + \tilde{\Phi}(P_F)\right) , \tag{11}$$

where $\tilde{\Phi}$ is the inverse function to Φ of (8). Thus, the single parameter d in (9) and (11) is a complete descriptor of performance for a linear input channel in figure 1. Furthermore, $\{s_k\}$ and $\{w_k\}$ are completely general in (9). Observe that the absolute scale of the reference cancels out in (9).

Matched Reference

If the local reference is matched to the received signal, then $w_k = As_k$ as in (4), and (9) yields the matched deflection parameter value

$$d_m = \frac{1}{\sigma_n}\left(\sum_k s_k^2\right)^{1/2} = \frac{E^{1/2}}{\sigma_n} , \tag{12}$$

where E is the received signal energy. Furthermore, this is the maximum possible value of d in (9) by choice of local reference $\{w_k\}$. Thus, the optimum performance of the linear-input correlator depends on the total received signal energy, and not on its fractionalization into individual samples $\{s_k\}$.

Clipped Reference

For this case, (4) yields $w_k = A\ \mathrm{sgn}(s_k)$, and (9) specializes to value

$$d_r = \frac{1}{K^{1/2}\ \sigma_n} \sum_k |s_k| \ . \tag{13}$$

This quantity depends on the specific fractionalization of the received signal energy into components $\{s_k\}$ and is, therefore, example-dependent. Its maximum value is again $E^{1/2}/\sigma_n$ as in (12), but only if all components are equal in magnitude. We will consider two particular signal examples in the rest of this section on the baseband correlator.

EXAMPLES

Example 1, Cosine Wave:

$$s_k = a \cos \phi_k, \quad \phi_k = 2\pi k/K \text{ for } 1 \le k \le K \ ; \quad a > 0 \ . \tag{14}$$

Example 2, Constant:

$$s_k = a \quad \text{for} \quad 1 \le k \le K \ ; \quad a > 0 \ . \tag{15}$$

For these two examples, the values of the matched deflection parameter in (12) become, respectively,

$$d_m^{(1)} = \left(\frac{K}{2}\right)^{1/2} \frac{a}{\sigma_n} , \quad d_m^{(2)} = K^{1/2} \frac{a}{\sigma_n} . \tag{16}$$

On the other hand, for a clipped reference, (13) yields corresponding values

$$d_r^{(1)} = \frac{1}{K^{1/2}} \sum_{k=1}^{K} \left|\cos(2\pi k/K)\right| \frac{a}{\sigma_n} = \begin{Bmatrix} 7.201\ a/\sigma_n & \text{for } K = 128 \\ 1.707\ a/\sigma_n & \text{for } K = 8 \end{Bmatrix} ,$$

$$d_r^{(2)} = K^{1/2} \frac{a}{\sigma_n} \quad \text{for all } K . \tag{17}$$

Since d is a complete descriptor of performance for the linear-input correlator, as given in (11), it is seen that for the cosine signal example 1, the clipped reference requires

$$-20 \log \left(\frac{d_r^{(1)}}{d_m^{(1)}}\right) = \begin{Bmatrix} -20 \log(7.201/8) = \ .91 \text{ dB} & \text{for } K = 128 \\ -20 \log(1.707/2) = 1.38 \text{ dB} & \text{for } K = 8 \end{Bmatrix} \tag{18}$$

additional input signal-to-noise ratio relative to the matched reference. On the other hand, constant signal example 2 requires a 0 dB difference, as seen by reference to (16) and (17). In general, (12) and (13) reveal a dB difference, due to clipping the reference, of

$$10 \log \left(K \frac{\sum_k s_k^2}{\left(\sum_k |s_k|\right)^2} \right) . \tag{19}$$

PROBABILITIES FOR NONLINEAR INPUT CHANNEL

Here, the nonlinearity g in the input channel of figure 1 is present; that is, $v_k = g(x_k)$ as in (3). Not yet specializing to the clipper of (2), we have system output

$$z = \sum_k w_k v_k = \sum_k w_k \; g(x_k) = \sum_k w_k \; g(s_k + n_k) \; , \qquad (20)$$

where signal $\{s_k\}$ and reference $\{w_k\}$ are also general.

The exact evaluation of the distribution of random variable z in (20) is difficult; accordingly we limit consideration to the case where K >> 1, meaning that z is approximately Gaussian. The p-th moment of the output of nonlinearity g, conditioned on input signal value s_k, is

$$\overline{g^p(s_k + n_k)} = \int dn \, \frac{1}{(2\pi)^{1/2} \, \sigma_n} \exp\left(-\frac{n^2}{2\sigma_n^2}\right) g^p(s_k + n) =$$

$$= \int dx \; \phi(x) \; g^p(s_k + \sigma_n x) \equiv G_p(s_k) \; , \qquad (21)$$

where we used the Gaussian character of noise $\{n_k\}$ and (8). Accordingly, the mean and variance of random variable z in (20) are

$$m_z = \bar{z} = \sum_k w_k \; G_1(s_k) \; ,$$

$$\sigma_n^2 = \sum_k w_k^2 \; \mathrm{Var}\big(g(s_k + n_k)\big) = \sum_k w_k^2 \left[G_2(s_k) - G_1^2(s_k)\right] , \qquad (22)$$

using the independent identically distributed property of noise $\{n_k\}$.

Then in a manner similar to (7), the detection and false alarm probabilities are given approximately by

$$P_D = \Phi\left(\frac{m_z - T}{\sigma_z}\right), \qquad P_F = \Phi\left(\frac{m_{zo} - T}{\sigma_{zo}}\right), \tag{23}$$

where T is the threshold, and the sub o designates setting the signal $\{s_k\}$ to zero in (21) and (22). Upon elimination of threshold T, the receiver operating characteristic is governed by the relation

$$P_D = \Phi\left(\Delta + \frac{\sigma_{zo}}{\sigma_z} \tilde{\Phi}(P_F)\right) , \tag{24}$$

where

$$\Delta = \frac{m_z - m_{zo}}{\sigma_z} = \frac{\sum_k w_k \left[G_1(s_k) - G_1(0)\right]}{\left(\sum_k w_k^2 \left[G_2(s_k) - G_1^2(s_k)\right]\right)^{1/2}} \tag{25}$$

is the appropriate deflection parameter in this case of a nonlinearly distorted input channel. However, Δ is not a complete descriptor of performance, since output z in (20) is not precisely Gaussian; however, for large numbers of samples, K, the receiver operating characteristic furnished by (24) should be a good approximation.

PROBABILITIES FOR CLIPPED-INPUT CORRELATOR

We now specialize the nonlinearity in figure 1 and (20) to the clipper of (2). Then (21) yields the first two moments

$$G_1(s) = \int dx\, \phi(x)\, \mathrm{sgn}(s + \sigma_n x) = 2\,\Phi\left(\frac{s}{\sigma_n}\right) - 1 ,$$

$$G_2(s) = \int dx\, \phi(x)\, \mathrm{sgn}^2(s + \sigma_n x) = 1 . \tag{26}$$

Substitution of these results in (22) then yields mean and variance

$$m_z = \sum_k w_k \left[2\,\Phi\left(\frac{s_k}{\sigma_n}\right) - 1 \right] ,$$

$$\sigma_z^2 = \sum_k w_k^2\, 4\,\Phi\left(\frac{s_k}{\sigma_n}\right) \Phi\left(-\frac{s_k}{\sigma_n}\right) . \tag{27}$$

Upon setting the signal $\{s_k\}$ to zero in (27), there follows

$$m_{zo} = 0 \quad , \quad \sigma_{zo}^2 = \sum_k w_k^2 . \tag{28}$$

Utilization of (27) and (28) in (24) and (25) yields the results for the clipped-input correlator, namely,

$$\Delta = \frac{\sum_k w_k \left[2\,\Phi\left(\frac{s_k}{\sigma_n}\right) - 1 \right]}{\left[\sum_k w_k^2\, 4\,\Phi\left(\frac{s_k}{\sigma_n}\right) \Phi\left(-\frac{s_k}{\sigma_n}\right) \right]^{1/2}} , \tag{29}$$

$$\frac{\sigma_{zo}}{\sigma_z} = \left(\frac{\sum_k w_k^2}{\sum_k w_k^2\, 4\,\Phi\left(\frac{s_k}{\sigma_n}\right) \Phi\left(-\frac{s_k}{\sigma_n}\right)} \right)^{1/2} . \tag{30}$$

Approximation for Small Signal-to-Noise Ratio

If the input signal-to-noise ratio in figure 1 is small, that is,

$$\frac{|s_k|}{\sigma_n} << 1 \text{ for all } k \ , \tag{31}$$

there follows from (8), the approximation

$$\Phi\left(\frac{s_k}{\sigma_n}\right) \cong \frac{1}{2} + (2\pi)^{-1/2} \frac{s_k}{\sigma_n} \ . \tag{32}$$

Then (29) simplifies to

$$\Delta = \left(\frac{2}{\pi}\right)^{1/2} \frac{\sum\limits_k w_k s_k}{\sigma_n \left(\sum\limits_k w_k^2\right)^{1/2}} = \left(\frac{2}{\pi}\right)^{1/2} d \ , \tag{33}$$

the last relation following directly from (9). And since (30) now reduces to $\sigma_{zo}/\sigma_z \cong 1$, (24) shows that Δ now is the sole parameter describing the receiver operating characteristic, under the assumptions of large K, number of samples, and small input signal-to-noise ratio.

Equation (33) reveals that the clipped-input system of figure 1 is degraded relative to the linear system by

$$20 \log \frac{d}{\Delta} = 20 \log\left(\frac{\pi}{2}\right)^{1/2} = 1.96 \text{ dB} \ , \tag{34}$$

regardless of the particular signal $\{s_k\}$ and regardless of the reference $\{w_k\}$ employed. Thus, clipping the input to the correlator in figure 1 causes a loss of 1.96 dB when K is large and the input signal-to-noise ratio is small, no matter what signal and reference are used.

Matched Reference

The deflection parameter Δ in (33) is maximized by choosing a matched reference, namely, $w_k = As_k$, thereby yielding

$$\Delta_m = \left(\frac{2}{\pi}\right)^{1/2} \frac{1}{\sigma_n} \left(\sum_k s_k^2\right)^{1/2} = \left(\frac{2}{\pi}\right)^{1/2} d_m \ . \tag{35}$$

The last identity follows from (12). Again, the performance of the clipped-input correlator depends only on the total received signal energy, and not on its fractionalization into components $\{s_k\}$.

Clipped Reference

For the clipped reference, with $w_k = A\ \mathrm{sgn}(s_k)$ from (4), (33) reduces to

$$\Delta_r = \left(\frac{2}{\pi}\right)^{1/2} \frac{1}{K^{1/2}\sigma_n} \sum_k |s_k| = \left(\frac{2}{\pi}\right)^{1/2} d_r \ , \tag{36}$$

the last relation following from (13). The loss relative to the linear-input clipped-reference correlator is again 1.96 dB, since (35) and (36) are special cases of (33) and (34).

EXAMPLE

For the cosine signal already considered in (14), the deflection parameters in (35) and (36) become

$$\Delta_m^{(1)} = \left(\frac{2}{\pi}\right)^{1/2}\left(\frac{K}{2}\right)^{1/2} \frac{a}{\sigma_n} = \left(\frac{2}{\pi}\right)^{1/2} d_m^{(1)} ,$$

$$\Delta_r^{(1)} = \begin{cases} 5.746\ a/\sigma_n & \text{for } K = 128 \\ 1.362\ a/\sigma_n & \text{for } K = 8 \end{cases} ; \qquad (37)$$

see (16) and (17). The first line reveals a 1.96 dB loss relative to the linear-input correlator, both with matched references. The second line indicates a loss dependent on the particular number of samples, K.

GRAPHICAL RESULTS

In figure 2, the receiver operating characteristics (ROC) for the linear-input correlator, as given by (11), are drawn in dotted lines, for the range (.001, .8) in false alarm probability and (.001, .999) in detection probability. Superposed as the jagged solid lines are the results of two simulations, each employing 30,000 trials*, for the linear-input correlator with K = 128 samples and for the cosine signal example of (14). For case A, $a/\sigma_n = .5$, whereas for case B, $a/\sigma_n = .25$. Reference to (16) reveals that these values correspond to deflections $d_m^{(1)} = 4$ and $d_m^{(1)} = 2$, respectively,

*A sample program is listed in the appendix.

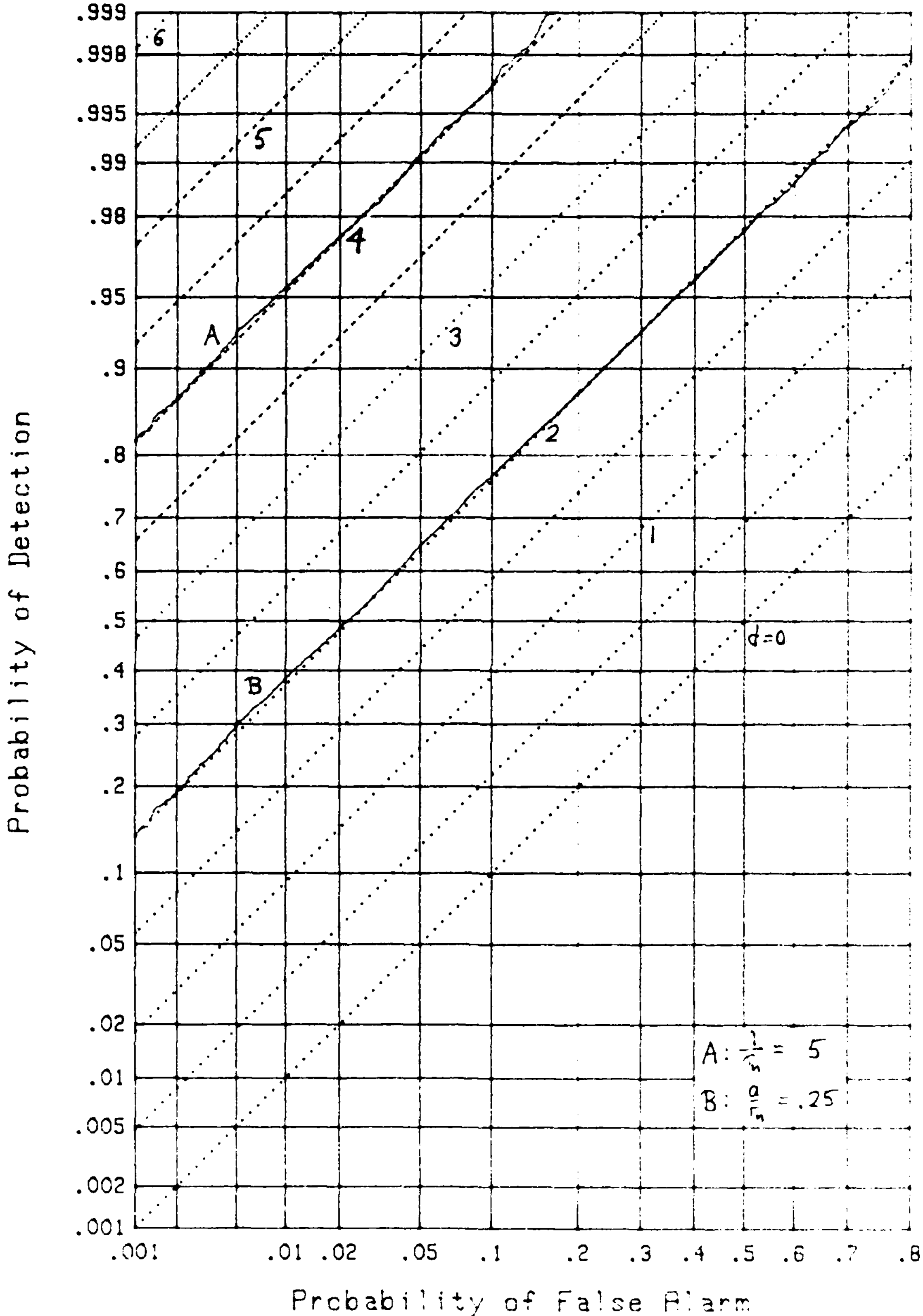

Figure 2. ROC for Baseband, Linear, K=128

and in fact, the simulations overlay these d-values very closely in figure 2, over the entire range shown. This agreement establishes the degree of confidence to be expected in the simulation results to follow.

In figure 3, the value of K is decreased to 8, while the values of a/σ_n are increased by a factor of 4. According to (16), this results in precisely the same d-values as above, and again, the simulations overlap the corresponding analytic results, even for this small value of K, as they should, since the correlator is linear.

In figure 4, K is increased to 128, but the reference is now clipped. According to the results in (17), we have

$$d_r^{(1)} = \left\{ \begin{matrix} 3.60 & \text{for } a/\sigma_n = .5 \\ 1.80 & \text{for } a/\sigma_n = .25 \end{matrix} \right\} \quad \text{for } K = 128 \ . \tag{38}$$

These values are borne out by the simulation for the cosine signal example in figure 4.

When K is decreased to 8, (17) now yields

$$d_r^{(1)} = \left\{ \begin{matrix} 3.41 & \text{for } a/\sigma_n = 2 \\ 1.71 & \text{for } a/\sigma_n = 1 \end{matrix} \right\} \quad \text{for } K = 8 \ . \tag{39}$$

The corresponding simulation results in figure 5 overlay these d values over the entire range plotted.

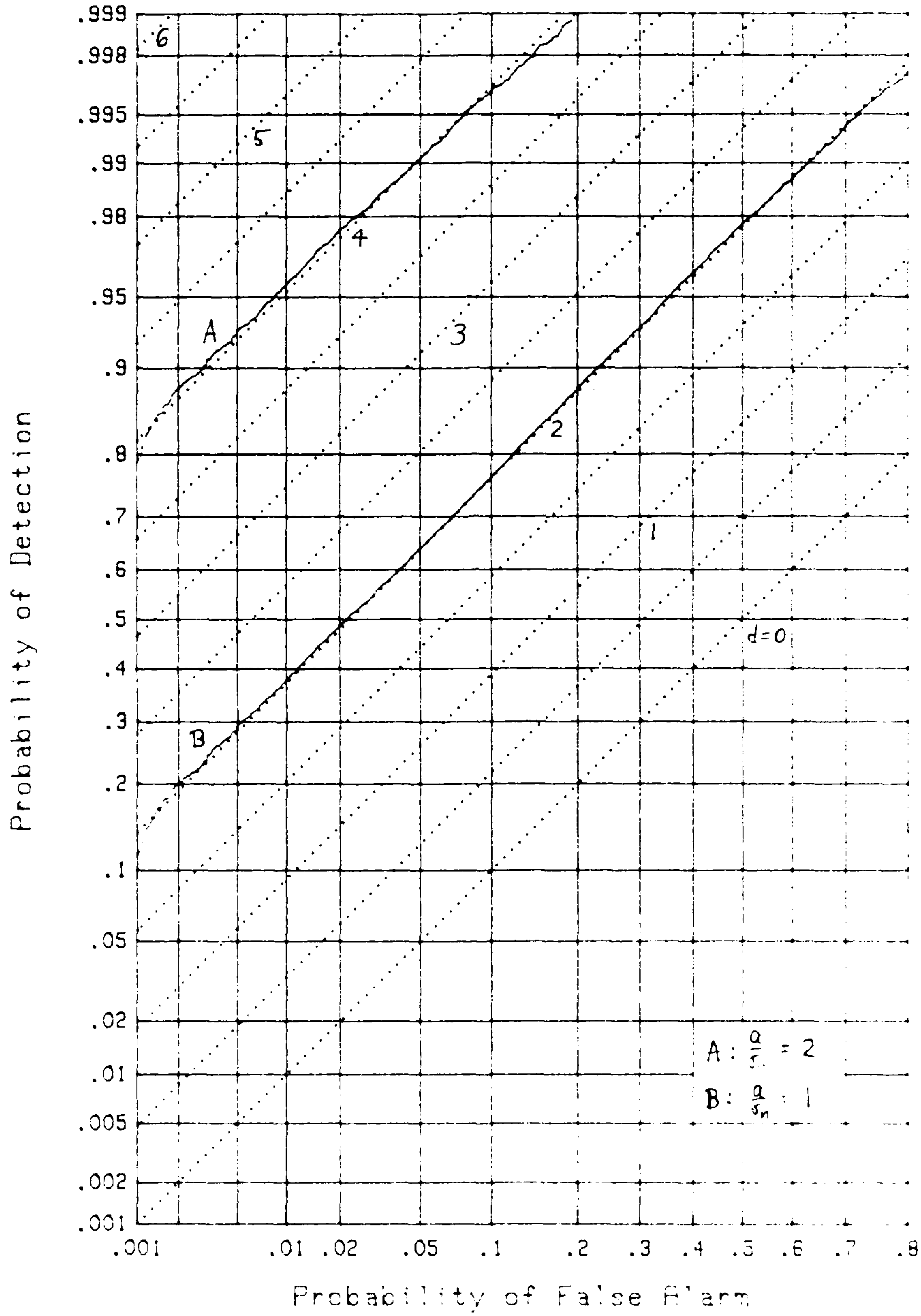

Figure 3. ROC for Baseband, Linear, K=8

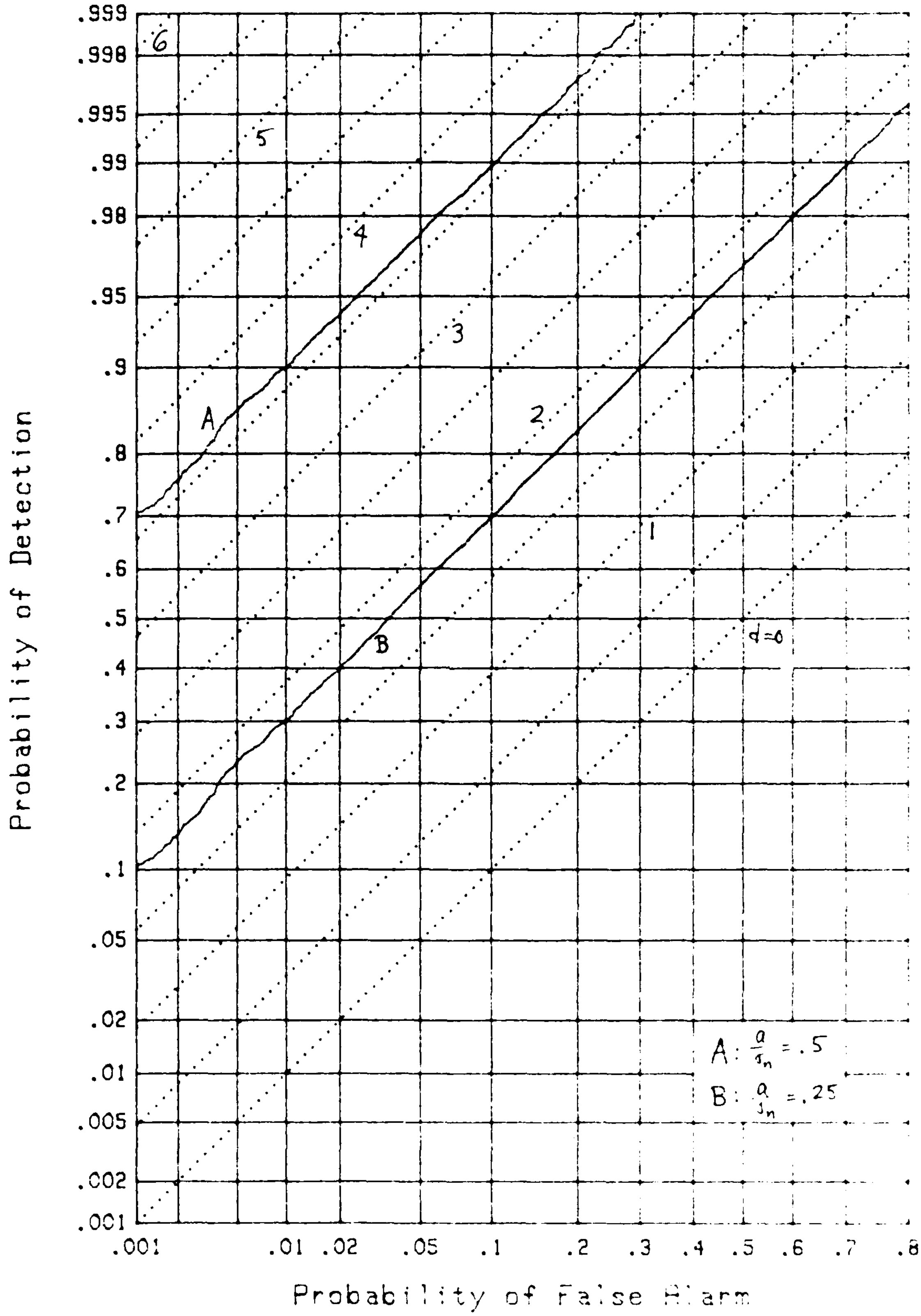

Figure 4. ROC for Baseband, Clip Reference, K=128

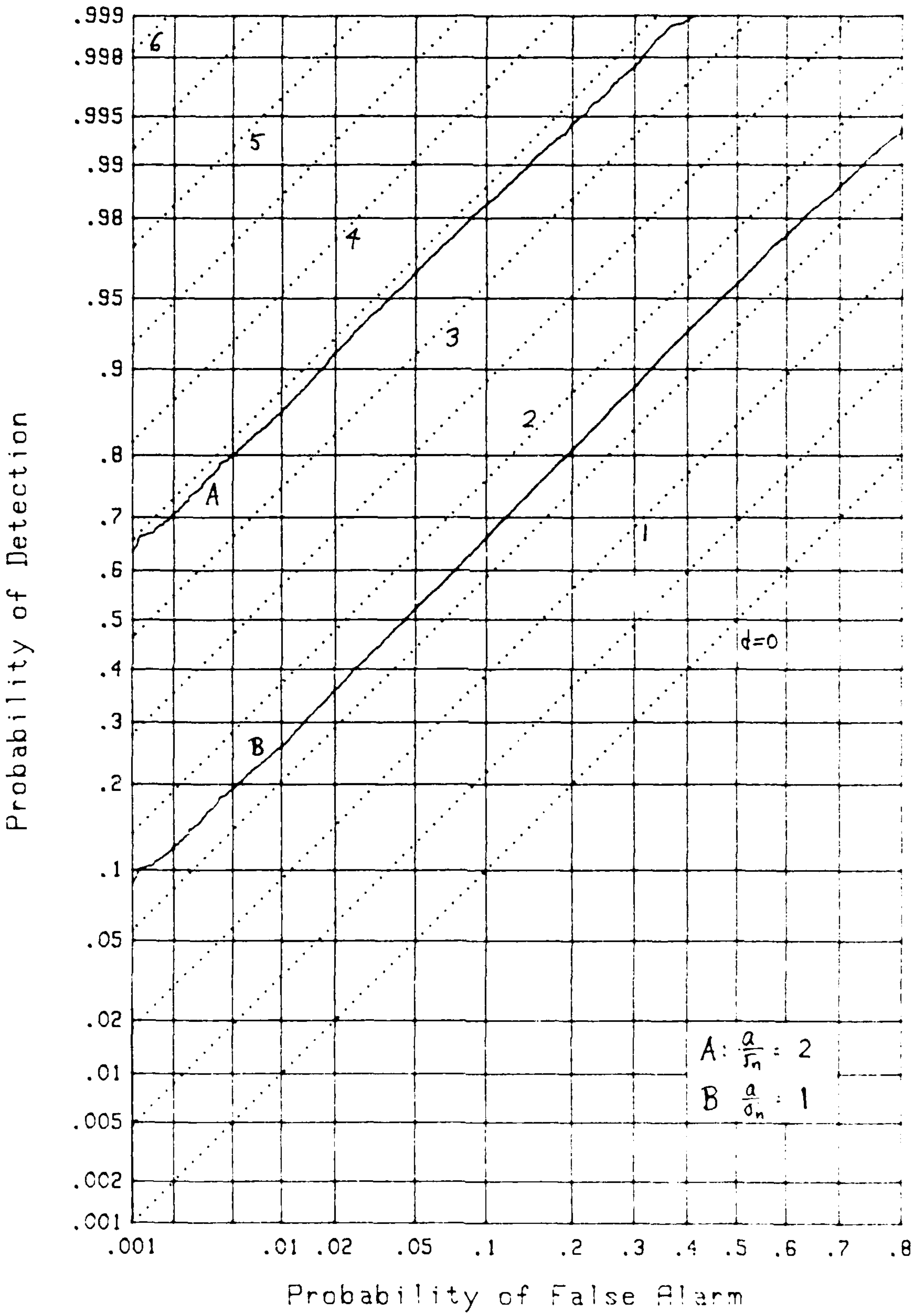

Figure 5. ROC for Baseband, Clip Reference, K=8

When the input is clipped, instead of the reference which is matched according to (35), the pertinent equation is the upper line of (37). There follows

$$\Delta_m^{(1)} = \left\{ \begin{array}{ll} 3.19 & \text{for } a/\sigma_n = .5 \\ 1.60 & \text{for } a/\sigma_n = .25 \end{array} \right\} \quad \text{for } K = 128\ . \tag{40}$$

Figure 6 correlates these values very well.

If K is decreased to 8, while a/σ_n is increased to 2 and 1, respectively, the same values result from the use of (37), as given in (40). The simulation results in figure 7 reveal that the actual performance does not meet those deflection values 3.19 and 1.60, except at the upper right ends of the curves. Two obvious reasons for the discrepancy are that K = 8 is not large enough to rely on the Gaussian approximation, and the input signal-to-noise ratios, a/σ_n = 2 or 1, are not small, as assumed in (31) et seq.

In an effort to circumvent the small input signal-to-noise ratio assumption made in (31), we returned to the more general results (29) and (30) and employed them in receiver operating characteristic (24). The values calculated for the matched reference $w_k = As_k$ were

$$\Delta = \left\{ \begin{array}{ll} 4.932 & \text{for } a/\sigma_n = 2 \\ 1.785 & \text{for } a/\sigma_n = 1 \end{array} \right\} \quad \text{for } K = 8\ ,$$

$$\frac{\sigma_{zo}}{\sigma_z} = \left\{ \begin{array}{ll} 2.298 & \text{for } a/\sigma_n = 2 \\ 1.258 & \text{for } a/\sigma_n = 1 \end{array} \right\} \quad \text{for } K = 8\ . \tag{41}$$

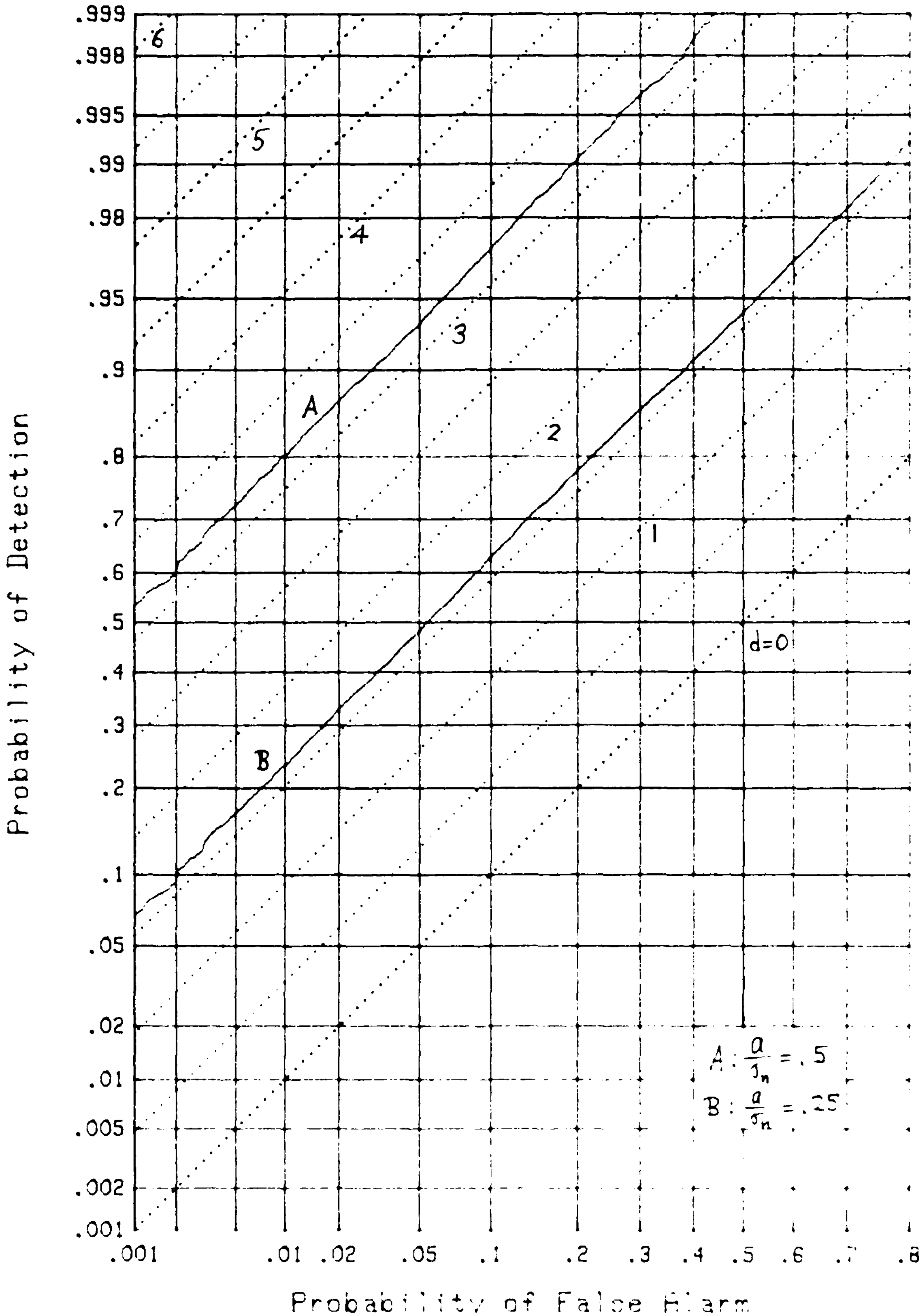

Figure 6. ROC for Baseband, Clip Input, K=128

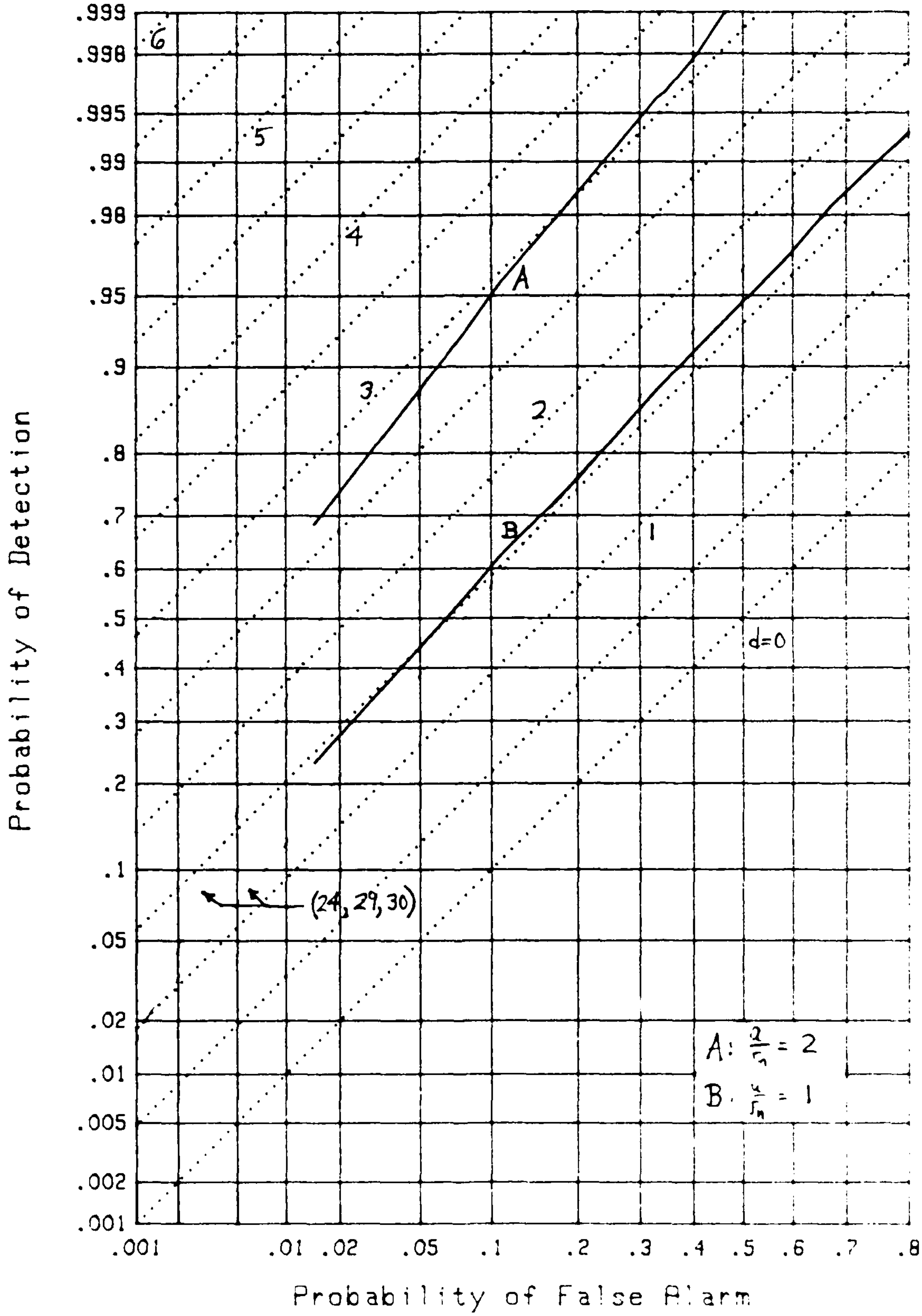

Figure 7. ROC for Baseband, Clip Input, K=8

These results are superposed in figure 7 with the label (24, 29, 30), and are seen to be poorer than those obtained via the low input signal-to-noise ratio results. However, this is felt to be a fortuitous circumstance.

When both the input and the reference are clipped, the simulation results for K = 128 are displayed in figure 8. The corresponding theory is furnished by (36) and yields the results for $\Delta_r^{(1)}$ already listed in (37). They become

$$\Delta_r^{(1)} = \left\{\begin{matrix} 2.873 & \text{for } a/\sigma_n = .5 \\ 1.436 & \text{for } a/\sigma_n = .25 \end{matrix}\right\} \quad \text{for } K = 128 \ , \qquad (42)$$

in excellent agreement with figure 8.

For the alternative situation with K = 8 and a/σ_n = 2 or 1, the appropriate values follow from (37) as

$$\Delta_r^{(1)} = \left\{\begin{matrix} 2.724 & \text{for } a/\sigma_n = 2 \\ 1.362 & \text{for } a/\sigma_n = 1 \end{matrix}\right\} \quad \text{for } K = 8 \ . \qquad (43)$$

These values do not furnish a good approximation to the corresponding simulation results depicted in figure 9, except at the upper right end. However, when we resort to the more accurate approach of (24), (29), (30), as discussed above, agreement is considerably better, although the slopes of the theoretical curves are steeper than those of the actual simulation results. A similar situation occurred in figure 7, although considerably worse there.

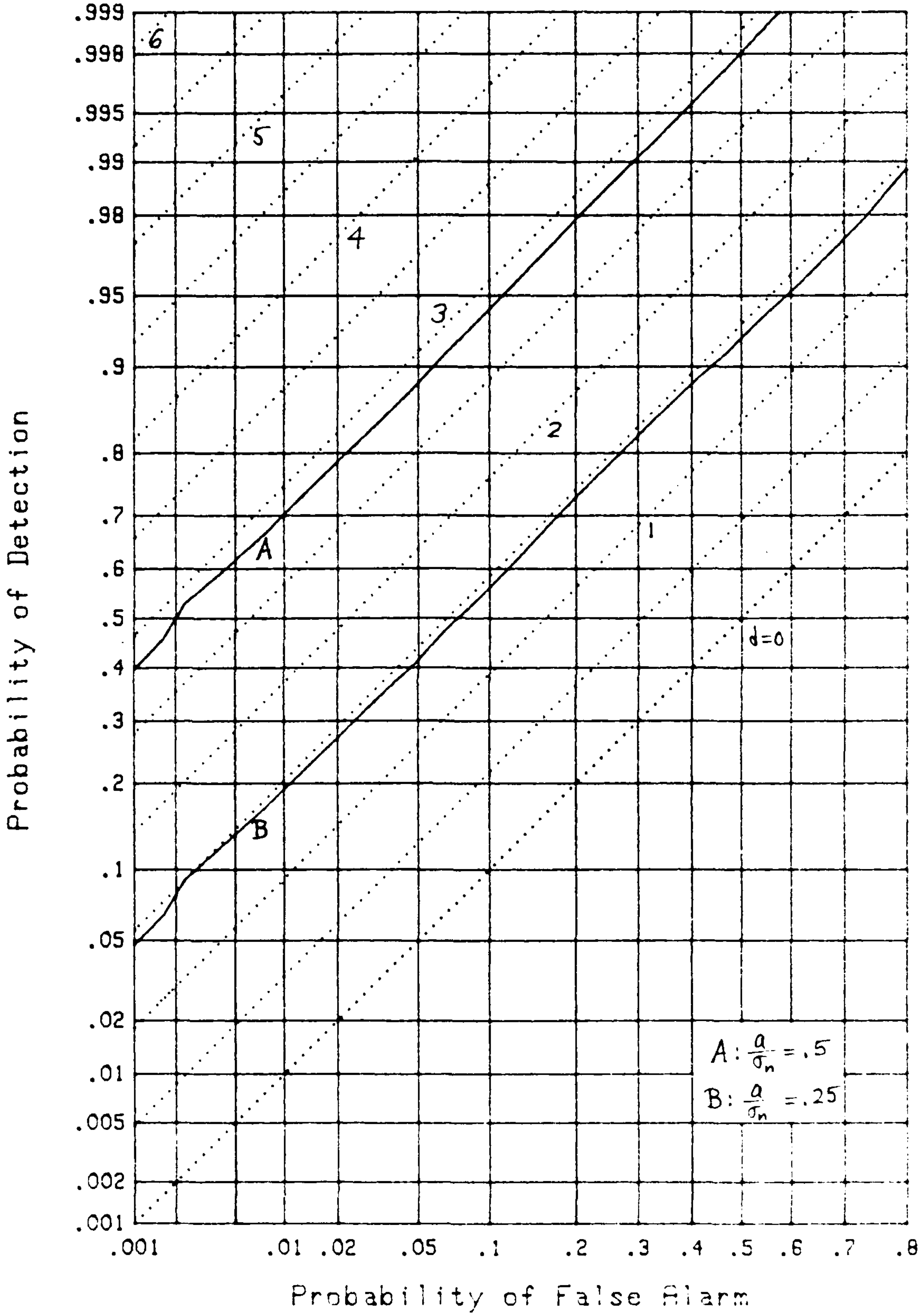

Figure 8. ROC for Baseband, Clip Both, K=128

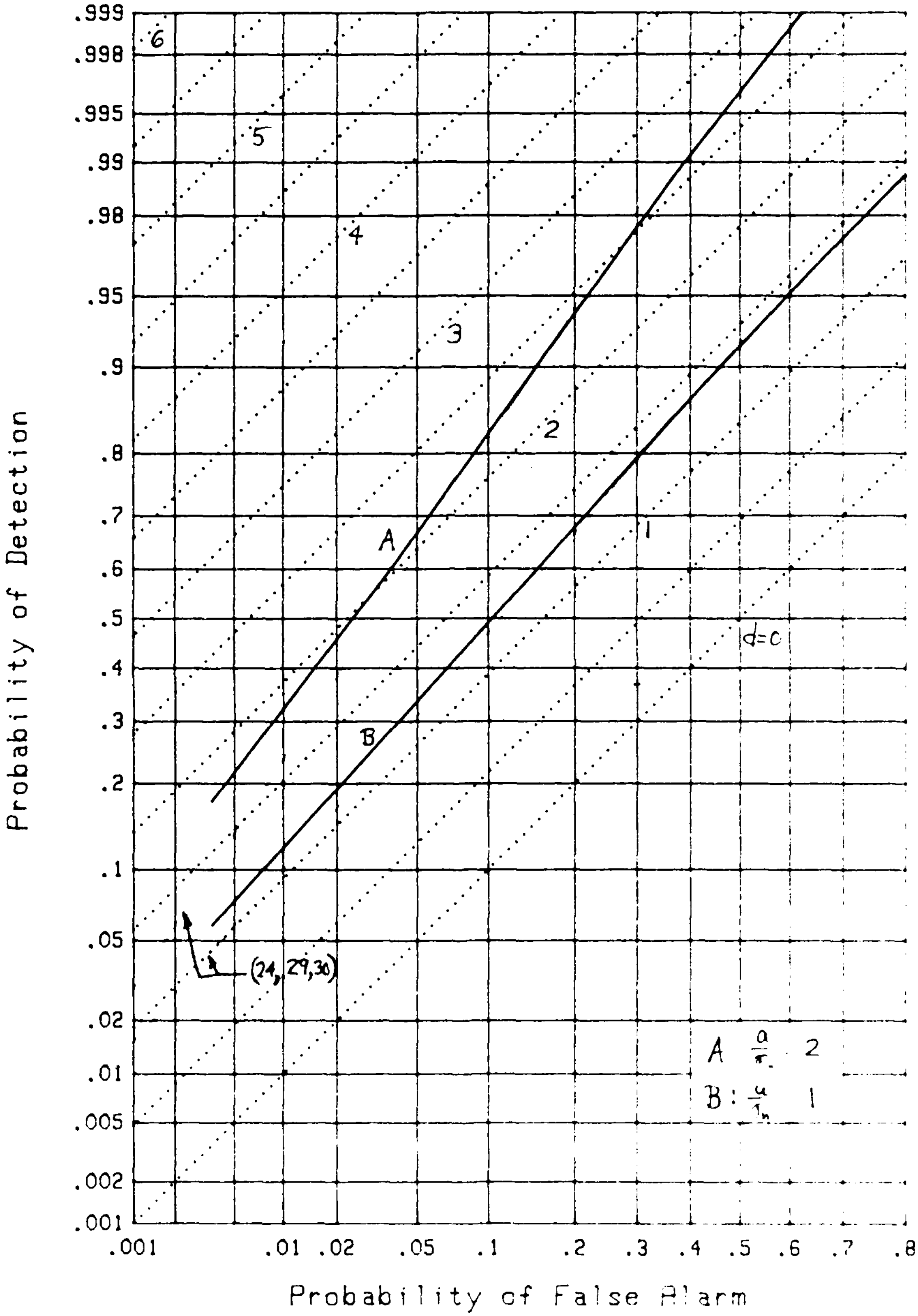

Figure 9. ROC for Baseband, Clip Both, K=8

NARROWBAND CORRELATOR

In this section, the correlator input and local reference are complex sampled processes, corresponding to the in-phase and quadrature components of the narrowband processes; see figure 10. The double arrows denote a pair of samples, as for the complex envelope of a narrowband process. It is presumed that any time delays or frequency shifts of the input signal have been compensated for, and we concentrate on the effects of clipping, at various locations, on the receiver operating characteristics of the correlator.

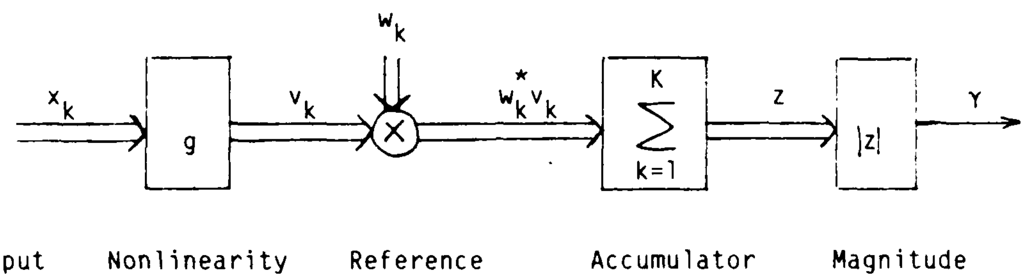

Figure 10. Narrowband Correlator

SYSTEM DESCRIPTION

The input to the correlator in figure 10 is

$$x_k = \begin{cases} n_k & \text{for } H_0 \\ s_k \exp(i\Theta) + n_k & \text{for } H_1 \end{cases}, \tag{44}$$

where $\{s_k\}$ is a deterministic known complex waveform, and Θ is a random variable. The phase shift Θ is independent of k; that is, the phase shift is constant but unknown over the observation interval K.

Additive noise $\{n_k\}$ is complex (circularly-symmetric) Gaussian with independent identically distributed components:

$$\overline{n_k} = 0 \qquad \text{for all } k \ ,$$

$$\left.\begin{aligned} \overline{n_k n_m} &= 0 \\ \overline{n_k n_m^*} &= 2\sigma_n^2 \, \delta_{km} \end{aligned}\right\} \text{ for all } k, m \ . \tag{45}$$

In particular, this means that $\overline{|n_k|^2} = 2\sigma_n^2$.

Expressing the noise in terms of its real and imaginary parts,

$$n_k = n_{kr} + i \, n_{ki} \ , \tag{46}$$

(45) yields the properties

$$\left.\begin{aligned} \overline{n_{kr}} &= \overline{n_{ki}} = 0 \\ \overline{n_{kr} n_{ki}} &= 0 \\ \overline{n_{kr}^2} &= \overline{n_{ki}^2} = \sigma_n^2 \end{aligned}\right\} \qquad \text{for all } k \ ,$$

$$\overline{n_{kr} n_{mr}} = \overline{n_{ki} n_{mi}} = \overline{n_{kr} n_{mi}} = 0 \qquad \text{for all } k \neq m \ . \tag{47}$$

Thus, σ_n^2 is the variance of each component of the received noise $\{n_k\}$.

The nonlinearity g in figure 10 is as given earlier in (2). However, since there are both in-phase and quadrature channels input to the nonlinearity, namely, x_{kr} and x_{ki}, its output is also complex:

$$v_k = g(x_{kr}) + i\, g(x_{ki}) = v_{kr} + i\, v_{ki} \, . \tag{48}$$

Thus, two nonlinearities are employed, one for each channel. When g is the clipper given by (2), output v_k takes on one of the four values $\pm 1 \pm i$, a 2-bit representation.

Local reference $\{w_k\}$ is also complex deterministic and directly related to the signal. Two examples are

$$w_k = \left\{ \begin{array}{ll} A\, s_k & \text{for linear reference} \\ A\, \mathrm{sgn}(s_{kr}) + i\, \mathrm{sgn}(s_{ki}) & \text{for clipped reference} \end{array} \right\} . \tag{49}$$

Again, two clippers are required in the reference channel, one for each component. This also results in a 2-bit representation for the reference. Complex scale factor A is irrelevant to the performance of the narrowband correlator.

The multiplier output in figure 10 is given by $w_k^* v_k$; that is, a conjugate is applied to the local reference. This complex quantity is summed over the observation interval of length K, yielding complex output

$$z = \sum_{k=1}^{K} w_k^* v_k = z_r + i\, z_i \, . \tag{50}$$

Finally, the magnitude of this quantity,

$$\gamma = |z| = \left(z_r^2 + z_i^2\right)^{1/2} , \tag{51}$$

is compared with a threshold for decision about signal absence (H_0) or presence (H_1).

PROBABILITIES FOR LINEAR-INPUT CHANNEL

In this subsection, we presume that the nonlinearity g in the input channel of figure 10 is absent; that is, from (2) and (48), $v_k = x_k$. Then accumulator output z in (50) becomes, for signal present,

$$z = \sum_k w_k^* v_k = \sum_k w_k^* x_k = \sum_k w_k^* \left(s_k \exp(i\theta) + n_k\right) = S + N , \tag{52}$$

where

$$S = \exp(i\theta) \sum_k w_k^* s_k , \quad N = \sum_k w_k^* n_k . \tag{53}$$

It should be observed that complex signal waveform $\{s_k\}$ and local reference $\{w_k\}$ are completely general at this point. That is, we have <u>not</u> restricted consideration to the examples given in (49) yet.

For a given fixed Θ, random variable z in (52) is complex Gaussian, since the operation of summation is linear in the noise variables $\{n_k\}$. We will find the probability of detection conditioned on a fixed value of Θ. The complex random variable N in (53) is Gaussian with moments

$$\overline{N} = \sum_k w_k^* \overline{n_k} = 0 ,$$

$$\overline{N^2} = \sum_{km} w_k^* w_m^* \overline{n_k n_m} = 0 ,$$

$$\overline{|N|^2} = \sum_{km} w_k^* w_m \overline{n_k n_m^*} = 2\sigma_n^2 \sum_k |w_k|^2 \equiv 2\sigma_N^2 . \tag{54}$$

Here we used the noise properties listed in (45). The statistics given in (54) hold true whether signal is present or not at the correlator input.

If we let N be expressed in terms of its real and imaginary parts,

$$N = N_r + i\, N_i , \tag{55}$$

the results of (54) translate into

$$\overline{N_r} = \overline{N_i} = 0 ,$$

$$\overline{N_r N_i} = 0 , \quad \overline{N_r^2} = \overline{N_i^2} = \sigma_N^2 . \tag{56}$$

Therefore, we can write the joint probability density function of the real and imaginary parts of z in (52) as

$$p(z_r,z_i) = \left(2\pi\sigma_N^2\right)^{-1} \exp\left[-\frac{\left(z_r - S_r\right)^2 + \left(z_i - S_i\right)^2}{2\sigma_N^2}\right], \tag{57}$$

for signal present.

The detection probability, for threshold T, is given by

$$P_D = \text{Prob}(\gamma > T) = \text{Prob}\left(\left(z_r^2 + z_i^2\right)^{1/2} > T\right) = \iint\limits_{\gamma>T} dz_r\, dz_i\, p(z_r,z_i) =$$

$$= \left(2\pi\sigma_N^2\right)^{-1} \iint\limits_{\gamma>T} dz_r\, dz_i\, \exp\left[-\frac{z_r^2 + z_i^2 - 2\left(S_r z_r + S_i z_i\right) + |S|^2}{2\sigma_N^2}\right] =$$

$$= (2\pi)^{-1} \int_{T/\sigma_n}^{\infty} d\rho\, \rho \int_{-\pi}^{\pi} d\phi\, \exp\left[-\frac{\rho^2}{2} + \frac{\rho}{\sigma_N}\left(S_r \cos\phi + S_i \sin\phi\right) + \frac{|S|^2}{2\sigma_N^2}\right] =$$

$$= \int_{T/\sigma_N}^{\infty} d\rho\, \rho\, \exp\left[-\frac{1}{2}\left(\rho^2 + d^2\right)\right] I_0(d\rho) = Q(d,\, T/\sigma_N)\ , \tag{58}$$

where we used in order: (51), (57), the substitution

$$z_r = \sigma_N\, \rho \cos\phi\ , \quad z_i = \sigma_N\, \rho \sin\phi\ , \tag{59}$$

[1; 8.431 3], and Marcum's Q-function [2; (1) for M = 1]. The parameter introduced in (58), namely,

$$d \equiv \frac{|S|}{\sigma_N} = \frac{\left|\sum\limits_k w_k^* s_k\right|}{\sigma_n \left(\sum\limits_k \left|w_k\right|^2\right)^{1/2}}\ , \tag{60}$$

is the analogue here, in the narrowband correlator, to the quantity (9) defined for the baseband correlator; we made use of (53) and (54) in (60).

Although the derivation in (54)-(58) was conditioned on a specific fixed value of Θ, the end result in (58) and (60) depends only on $|S|$ which is independent of Θ. Therefore, the detection probability of the narrowband correlator is independent of whatever Θ is, and (58) is also the unconditional detection probability, there being no need to average over Θ; its exact probability density function is irrelevant.

The false alarm probability is obtained from (58) and (60) by setting the signal $\{s_k\}$ to zero, and using [2, (2)]:

$$P_F = Q(0, T/\sigma_N) = \exp\left(-\frac{T^2}{2\sigma_N^2}\right). \tag{61}$$

Eliminating T/σ_N from (58) and (61), we obtain the operating characteristic in the form

$$P_D = Q\left(d, (-2\ln P_F)^{1/2}\right). \tag{62}$$

Thus, deflection parameter d in (60) is a complete descriptor of performance for the linear-input narrowband correlator in figure 10. Furthermore, signal $\{s_k\}$ and local reference $\{w_k\}$ are completely general in (60).

Matched Reference

If the local reference is matched to the received signal, then $w_k = As_k$ as in (49), and (60) yields for the matched deflection parameter the value

$$d_m = \frac{1}{\sigma_n}\left(\sum_k |s_k|^2\right)^{1/2} = \frac{(2E)^{1/2}}{\sigma_n} , \tag{63}$$

where E is the energy of the received real signal. Furthermore, this is the maximum possible value of d in (60) by choice of local reference $\{w_k\}$. Thus, the optimum performance of the linear-input narrowband correlator depends on the total received signal energy, and not on its fractionalization into individual components $\{s_k\}$.

Clipped Reference

Since (60) and (62) hold for any reference, we can specialize it to the clipped case given in (49), namely,

$$w_k = A\left[\mathrm{sgn}(s_{kr}) + i\ \mathrm{sgn}(s_{ki})\right] . \tag{64}$$

Substitution in (60) yields

$$d_r = \sigma_n^{-1}(2K)^{-1/2}\left|\sum_k \left[\mathrm{sgn}(s_{kr}) - i\ \mathrm{sgn}(s_{ki})\right]\left[s_{kr} + i\ s_{ki}\right]\right| . \tag{65}$$

This quantity depends on the specific fractionalization of the received signal energy into components and is, therefore, example-dependent. Its maximum value is again $(2E)^{1/2}/\sigma_n$ as in (63), but only if all components $\{s_k\}$ are the same complex constant. The degradation of d_r relative to d_m

depends on the specific signal $\{s_k\}$. We will consider two particular signal examples in the rest of this section on the narrowband correlator.

EXAMPLES

Example 1, Phase-modulated tone:

$$s_k = a \exp(i\phi_k), \quad \phi_k = 2\pi k/K \text{ for } 1 \le k \le K; \quad a > 0 \,. \tag{66}$$

Example 2, Pure tone:

$$s_k = a \exp(i\phi) \text{ for } 1 \le k \le K; \quad a > 0, \quad \phi \text{ constant} \,. \tag{67}$$

For these two examples, the values of the matched deflection parameter in (63) become, respectively,

$$d_m^{(1)} = d_m^{(2)} = K^{1/2} \frac{a}{\sigma_n} \,. \tag{68}$$

On the other hand, for a clipped reference, (65) yields the corresponding values

$$d_r^{(1)} = \begin{Bmatrix} 10.187\ a/\sigma_n & \text{for } K = 128 \\ 2.613\ a/\sigma_n & \text{for } K = 8 \end{Bmatrix},$$

$$d_r^{(2)} = K^{1/2} \frac{a}{\sigma_n} \qquad \text{for all } K \,. \tag{69}$$

Since d in (60) and (62) is a complete descriptor of performance for the linear-input narrowband correlator, it is seen that for the phase-modulated tone of example 1, the clipped reference requires

$$-20 \log\left(\frac{d_r^{(1)}}{d_m^{(1)}}\right) = \begin{cases} -20 \log\left(10.187/\sqrt{128}\right) = .91 \text{ dB} & \text{for } K = 128 \\ -20 \log\left(2.613/\sqrt{8}\right) = .69 \text{ dB} & \text{for } K = 8 \end{cases}$$

additional input signal-to-noise ratio relative to the matched reference. On the other hand, the pure tone signal example 2 requires a 0 dB difference, as seen by reference to (68) and (69). In general, (63) and (65) reveal a dB difference, due to clipping the reference, of

$$10 \log\left(2K \frac{\sum_k |s_k|^2}{\left|\sum_k \left[\operatorname{sgn}(s_{kr}) - i \operatorname{sgn}(s_{ki})\right]\left[s_{kr} + i s_{ki}\right]\right|^2}\right). \tag{70}$$

MOMENTS FOR NONLINEAR INPUT CHANNEL

In this subsection, the nonlinearity g in the input channel of figure 10 is present; that is, v_k is given by (48) in terms of two nonlinearities, one each in the in-phase and quadrature channels. For a general nonlinearity g, the accumulator output is

$$z = \sum_k w_k^* v_k = \sum_k w_k^* \left[g(x_{kr}) + i\, g(x_{ki})\right] , \tag{71}$$

where input

$$x_k = s_k \exp(i\theta) + n_k \equiv t_k + n_k . \tag{72}$$

Signal $\{s_k\}$ and reference $\{w_k\}$ are also general at this point. Random variable θ is held fixed for the moment. Substituting (72) in (71), there follows

$$z = \sum_k w_k^* \left[g(t_{kr} + n_{kr}) + i\, g(t_{ki} + n_{ki}) \right] . \tag{73}$$

We now assume that K, the number of samples accumulated, is large, so that z is well approximated as a complex Gaussian random variable. In that case, we can concentrate on the two lowest-order moments of z. The p-th moment of the real output of one of the nonlinearities is

$$\overline{g^p(t_{kr} + n_{kr})} = \int dn \, \frac{1}{(2\pi)^{1/2}\sigma_n} \exp\left(-\frac{n^2}{2\sigma_n^2}\right) g^p(t_{kr} + n) =$$

$$= \int dx \, \phi(x) \, g^p(t_{kr} + \sigma_n x) \equiv G_p(t_{kr}) , \tag{74}$$

where we used the Gaussian character of the noise, (47), and (8). In a similar manner,

$$\overline{g^p(t_{ki} + n_{ki})} = G_p(t_{ki}) . \tag{75}$$

The mean of complex random variable z in (73) then follows easily as

$$m_z = \bar{z} = \sum_k w_k^* \left[G_1(t_{kr}) + i\, G_1(t_{ki}) \right] . \tag{76}$$

To determine the second central moments of z, we combine (73) and (76) in the form

$$z - \bar{z} = \sum_k (\alpha_k + \beta_k) , \tag{77}$$

where

$$\alpha_k = w_k^*\left[g(t_{kr} + n_{kr}) - G_1(t_{kr})\right] ,$$

$$\beta_k = i\, w_k^*\left[g(t_{ki} + n_{ki}) - G_1(t_{ki})\right] . \tag{78}$$

From (47), every random variable α_k is independent of every α_m for $m \neq k$, and independent of every β_m for all m. A similar property holds for every random variable β_k. In addition, $\overline{\alpha_k} = \overline{\beta_k} = 0$. It then follows that

$$\overline{(z - \bar{z})^2} = \overline{\sum_{km} (\alpha_k + \beta_k)(\alpha_m + \beta_m)} = \sum_k \left(\overline{\alpha_k^2} + \overline{\beta_k^2}\right) =$$

$$= \sum_k w_k^{*2}\left[G_2(t_{kr}) - G_1^2(t_{kr}) - G_2(t_{ki}) + G_1^2(t_{ki})\right] ,$$

$$\overline{\left|z - \bar{z}\right|^2} = \sum_{km} \overline{(\alpha_k + \beta_k)\left(\alpha_m^* + \beta_m^*\right)} = \sum_k \left(\overline{\left|\alpha_k\right|^2} + \overline{\left|\beta_k\right|^2}\right) =$$

$$= \sum_k \left|w_k\right|^2\left[G_2(t_{kr}) - G_1^2(t_{kr}) + G_2(t_{ki}) - G_1^2(t_{ki})\right] . \tag{79}$$

PROBABILITIES FOR CLIPPED-INPUT CORRELATOR

We now specialize these results to the case of the clipper $g(x) = \mathrm{sgn}(x)$. Then (74) yields

$$G_1(t) = \int dx\ \phi(x)\ \mathrm{sgn}(t + \sigma_n x) = 2\,\Phi(t/\sigma_n) - 1 ,$$

$$G_2(t) = \int dx\ \phi(x)\ \mathrm{sgn}^2(t + \sigma_n x) = 1 . \tag{80}$$

We further restrict attention to the case of small input signal-to-noise ratio in figure 10, that is,

$$\frac{|s_k|}{\sigma_n} << 1 \text{ for all } k \ , \tag{81}$$

in which case (80) yields, with the help of (32),

$$G_1(t_{kr}) \cong \left(\frac{2}{\pi}\right)^{1/2} \frac{t_{kr}}{\sigma_n} \ , \quad G_1(t_{ki}) \cong \left(\frac{2}{\pi}\right)^{1/2} \frac{t_{ki}}{\sigma_n} \ . \tag{82}$$

Utilization of these approximations in (76) yields mean

$$m_z = \left(\frac{2}{\pi}\right)^{1/2} \sum_k w_k^* \frac{t_{kr} + i\, t_{ki}}{\sigma_n} = \left(\frac{2}{\pi}\right)^{1/2} \frac{\exp(i\Theta)}{\sigma_n} \sum_k w_k^* s_k \ , \tag{83}$$

where we used (72).

Similarly, (79) reduces to

$$\overline{(z - \bar{z})^2} = \frac{2}{\pi} \sum_k w_k^{*2} \frac{t_{ki}^2 - t_{kr}^2}{\sigma_n^2} = -\frac{2}{\pi} \sum_k w_k^{*2} \operatorname{Re}\left(\frac{s_k^2}{\sigma_n^2} e^{i2\Theta}\right) \ ,$$

$$\overline{|z - \bar{z}|^2} = \sum_k |w_k|^2 \left[2 - \frac{2}{\pi} \frac{t_{kr}^2 + t_{ki}^2}{\sigma_n^2}\right] = \sum_k |w_k|^2 \left[2 - \frac{2}{\pi} \frac{|s_k|^2}{\sigma_n^2}\right] . \tag{84}$$

By the small input signal-to-noise ratio assumption in (81), it can be seen that the magnitude of $\overline{(z - \bar{z})^2}$ in (84) is much smaller than $\overline{|z - \bar{z}|^2}$. In this case, we have the good approximations

$$\overline{(z - \bar{z})^2} \cong 0 ,$$

$$\overline{\left|z - \bar{z}\right|^2} \cong 2 \sum_k \left|w_k\right|^2 \equiv 2\sigma_z^2 . \tag{85}$$

Observe, that to this order of approximation, all dependence of these moments on signal $\{s_k\}$ has disappeared.

Thus, for signal present, the joint probability density function of the real and imaginary parts of z in (71) is

$$p(z_r, z_i) = \left(2\pi\sigma_z^2\right)^{-1} \exp\left[- \frac{(z_r - m_{zr})^2 + (z_i - m_{zi})^2}{2\sigma_z^2}\right] . \tag{86}$$

Then in an identical manner to that developed in (58), the detection probability is, for threshold T,

$$P_D = \mathrm{Prob}(\gamma > T) = \mathrm{Prob}\left(\left(z_r^2 + z_i^2\right)^{1/2} > T\right) =$$

$$= Q(\Delta, T/\sigma_z) , \tag{87}$$

where

$$\Delta \equiv \frac{|m_z|}{\sigma_z} = \left(\frac{2}{\pi}\right)^{1/2} \frac{\left|\sum_k w_k^* s_k\right|}{\sigma_n \left(\sum_k \left|w_k\right|^2\right)^{1/2}} . \tag{88}$$

Notice that random variable Θ, which was present in (72) and (83), has now disappeared in Δ and detection probability P_D. Also Δ is precisely equal to d in (60) except for a scale factor of $(2/\pi)^{1/2}$. Thus, the clipped-input correlator is degraded relative to the linear-input correlator by 1.96 dB, measured at the system inputs, <u>regardless</u> of the signal $\{s_k\}$ and reference $\{w_k\}$.

If we set the signal to zero in (87) and (88), we obtain false alarm probability

$$P_F = Q(0, T/\sigma_z) = \exp\left(-\frac{T^2}{2\sigma_z^2}\right), \tag{89}$$

where σ_z is the common variable defined in (85) and used in (86)-(88). Eliminating threshold T from (87) and (89), we obtain the receiver operating characteristic as

$$P_D = Q\left(\Delta, (-2\ln P_F)^{1/2}\right) . \tag{90}$$

The parameter Δ defined in (88) is a good descriptor of performance when the assumptions of large K and small input signal-to-noise ratio are met.

Matched Reference

The deflection parameter Δ in (88) is maximized by choosing a matched reference, that is, $w_k = As_k$, thereby yielding

$$\Delta_m = \left(\frac{2}{\pi}\right)^{1/2} \frac{1}{\sigma_n}\left(\sum_k |s_k|^2\right)^{1/2} = \left(\frac{2}{\pi}\right)^{1/2} d_m . \tag{91}$$

The last relation follows upon reference to (63). It is seen that the performance of the clipped-input narrowband correlator depends only on the total received signal energy in this case.

Clipped Reference

For the clipped reference, we again make the choice delineated in (64). The result for the corresponding value of deflection parameter Δ in (88) is

$$\Delta_r = \left(\frac{2}{\pi}\right)^{1/2} d_r , \tag{92}$$

where d_r is given by (65). Thus, the degradation of Δ_r, relative to matched value Δ_m above, depends on the specific choice of signal waveform selected.

EXAMPLE

For the phase-modulated tone presented in (66), (91) yields

$$\Delta_m^{(1)} = \left(\frac{2}{\pi}\right)^{1/2} K^{1/2} \frac{a}{\sigma_n} = \left(\frac{2}{\pi}\right)^{1/2} d_m^{(1)} , \tag{93}$$

a 1.96 dB degradation relative to the linear-input narrowband correlator with a matched reference. On the other hand, (92) and (69) yield

$$\Delta_r^{(1)} = \begin{cases} 8.128\ a/\sigma_n & \text{for } K = 128 \\ 2.085\ a/\sigma_n & \text{for } K = 8 \end{cases} , \tag{94}$$

giving a loss that depends on the particular number of samples, K.

GRAPHICAL RESULTS

In figure 11, the receiver operating characteristics (ROC) for the linear-input narrowband correlator, as governed by (62), are drawn in dotted lines, for the range (.001, .8) in false alarm probability and (.001, .999) in detection probability. These are no longer parallel straight lines, as they were for the baseband single-channel case in figures 1-9, but bend downward as the false alarm probability increases (that is, as the threshold decreases).

Superposed as the jagged solid lines are the results of two simulations, each employing 30,000 trials*, for the linear-input narrowband correlator with K = 128 samples and for the phase-modulated tone example of (66). For case A, $a/\sigma_n = \sqrt{2}/4$, whereas for case B, $a/\sigma_n = \sqrt{2}/8$. These values were chosen so that the deflections would take on the values $d_m^{(1)} = 4$ and $d_m^{(1)} = 2$, respectively, as may be seen by reference to (68). The overlay of simulation and theory is excellent in figure 11 over the entire range of probabilities plotted, and establish the degree of confidence to be expected in the simulation results to follow.

In figure 12, K is reduced to 8, while the values of a/σ_n are increased by a factor of 4, thereby realizing the same d-values as above, according to (68). The agreement of results is again very good, except for the upper end of the $a/\sigma_n = \sqrt{2}$ curve, where the simulation result is low. This particular

---

*A sample program is listed in the appendix.

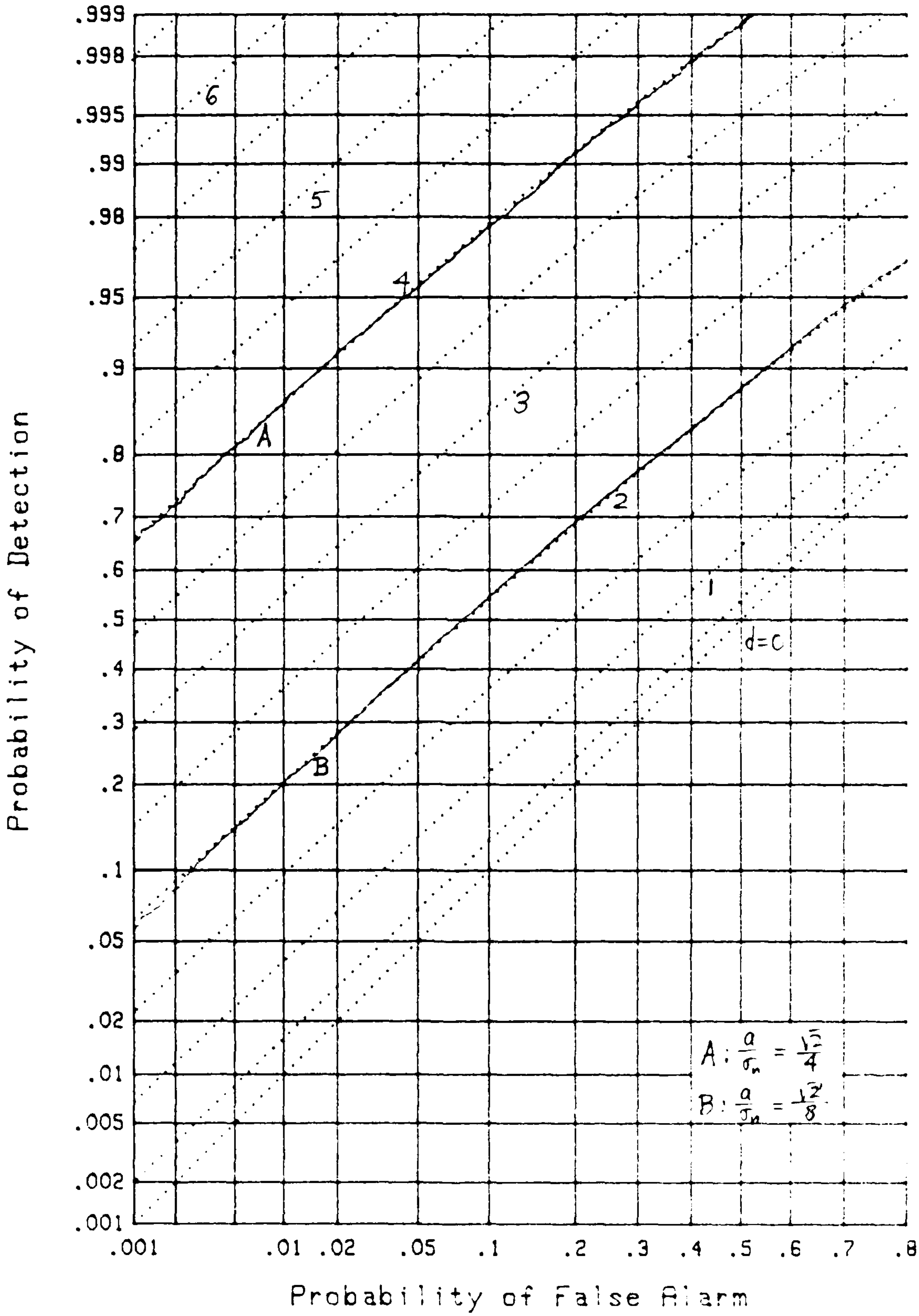

Figure 11. ROC for Narrowband, Linear, K=128

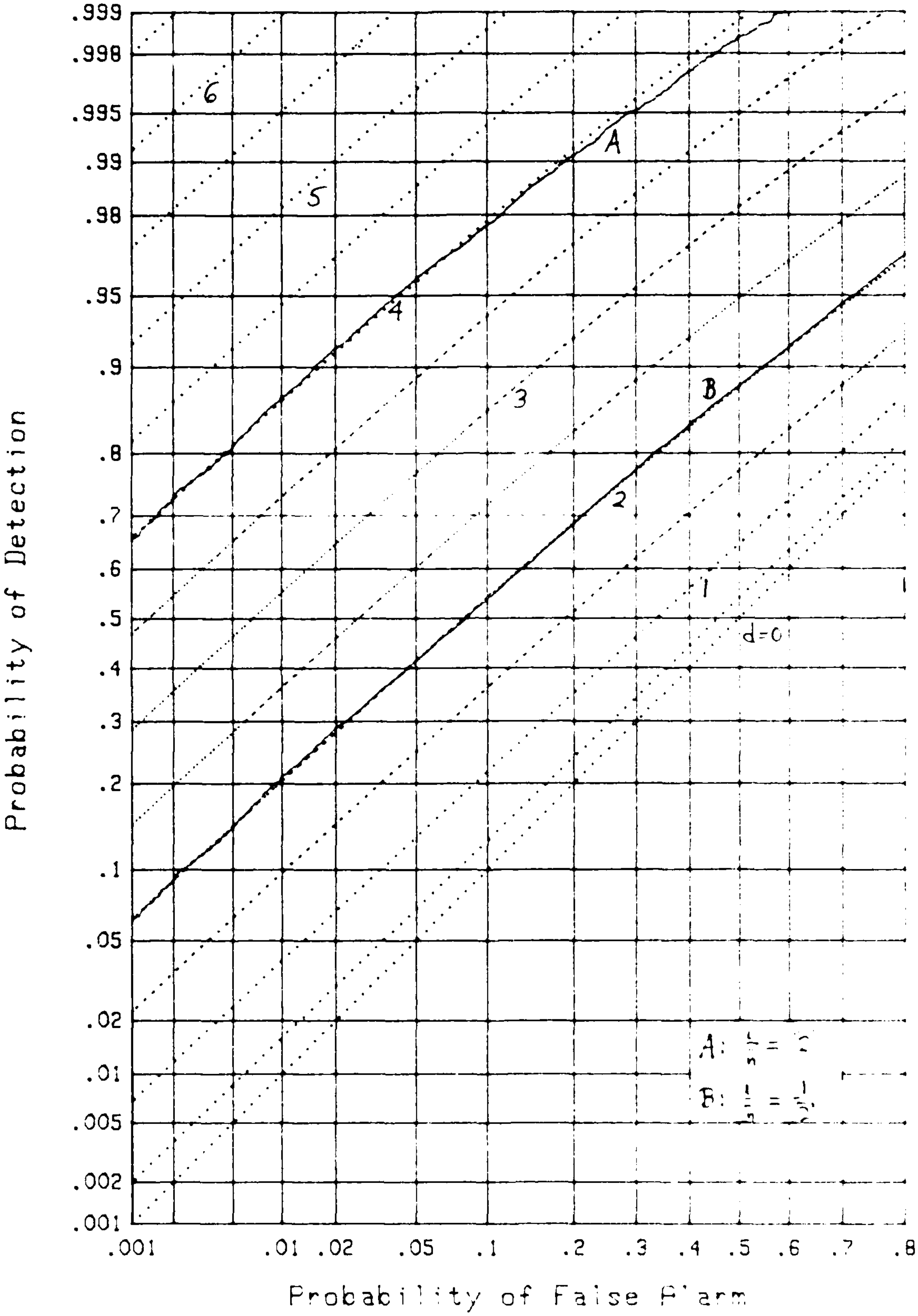

Figure 12. ROC for Narrowband, Linear, K=8

simulation is atypical; a re-run with a different set of 30,000 independent trials yielded good agreement over the entire range plotted. However, it does serve to illustrate a pitfall of simulation results, even when based on 30,000 trials, as these results are; it is possible to get a systematic error in the receiver operating characteristic, especially on the tails of the distributions.

In figure 13, K is increased back to 128, but the reference is now clipped. According to (69), we now have

$$d_r^{(1)} = \begin{Bmatrix} 3.60 \text{ for } a/\sigma_n = \sqrt{2}/4 \\ 1.80 \text{ for } a/\sigma_n = \sqrt{2}/8 \end{Bmatrix} \text{ for } K = 128 , \tag{95}$$

which values are borne out by the simulation results in figure 13.

When K is decreased to 8, (69) now yields

$$d_r^{(1)} = \begin{Bmatrix} 3.70 \text{ for } a/\sigma_n = \sqrt{2} \\ 1.85 \text{ for } a/\sigma_n = 1/\sqrt{2} \end{Bmatrix} \text{ for } K = 8 . \tag{96}$$

These results are confirmed by the plots in figure 14.

When the input to the narrowband correlator is clipped, instead of the reference (which is matched according to (91)), the pertinent equation is (93). There follows

$$\Delta_m^{(1)} = \begin{Bmatrix} 3.19 \text{ for } a/\sigma_n = \sqrt{2}/4 \\ 1.60 \text{ for } a/\sigma_n = \sqrt{2}/8 \end{Bmatrix} \text{ for } K = 128 . \tag{97}$$

Figure 15 corroborates these predictions.

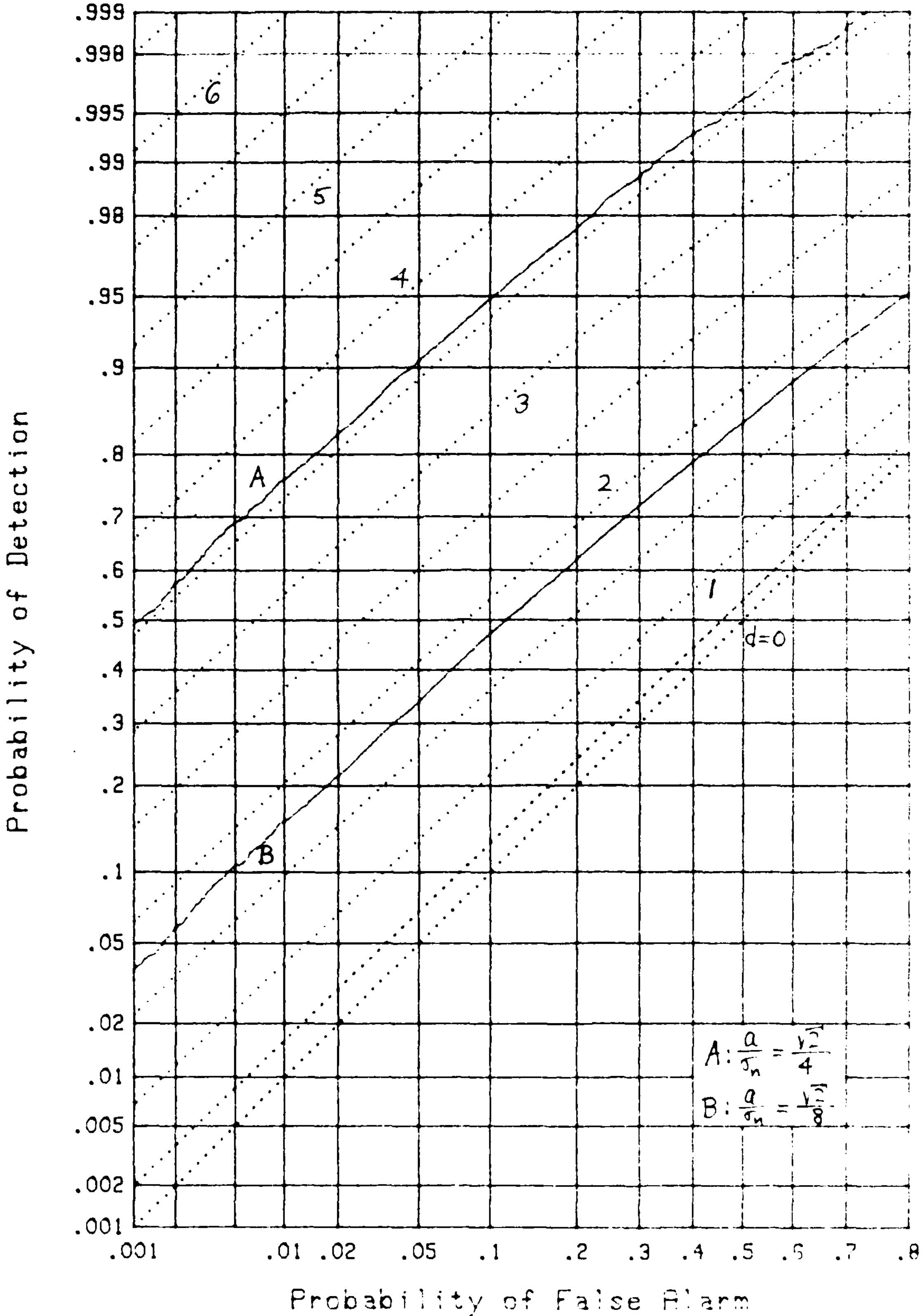

Figure 13. ROC for Narrowband, Clip Reference, K=128

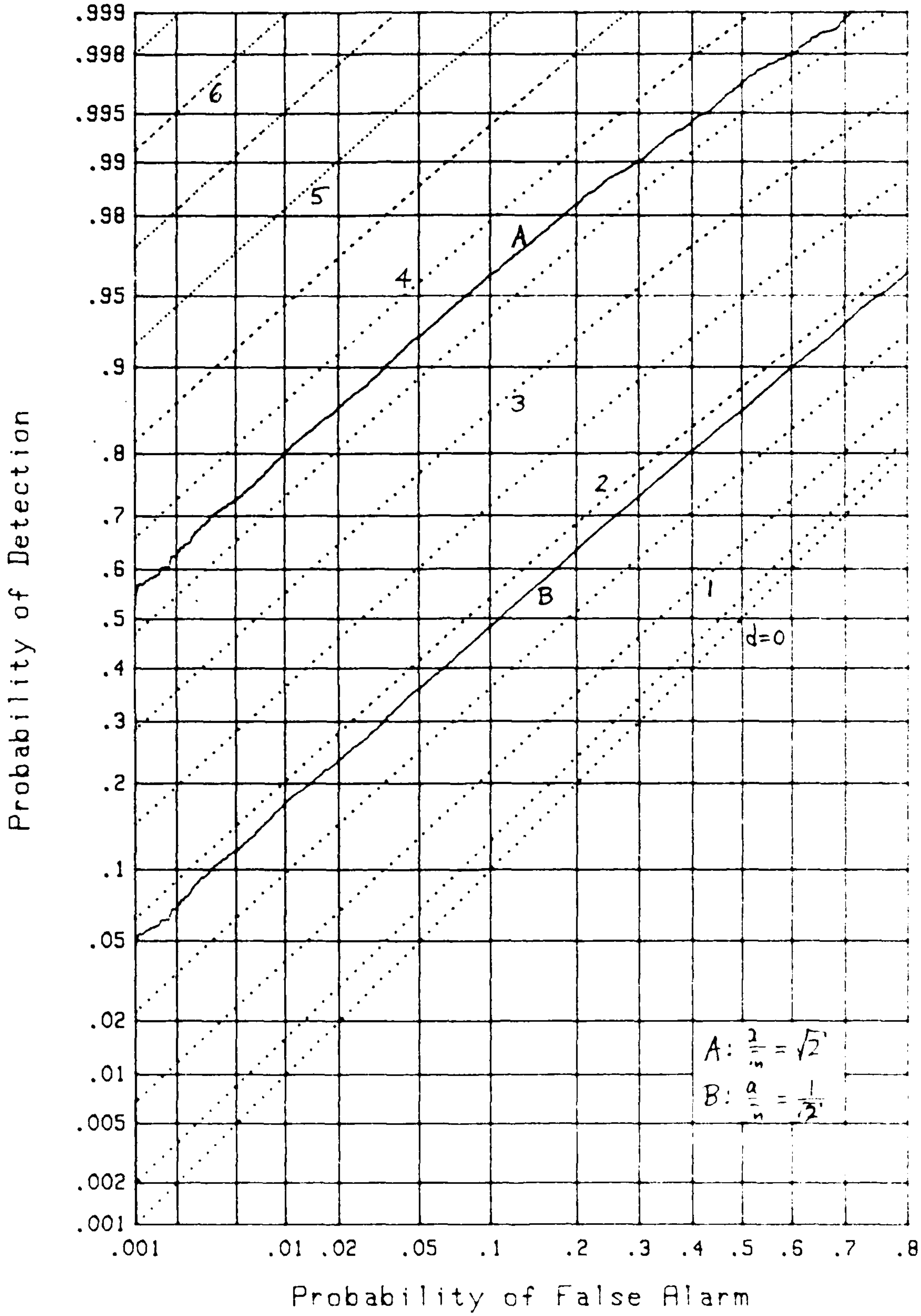

Figure 14. ROC for Narrowband, Clip Reference, K=8

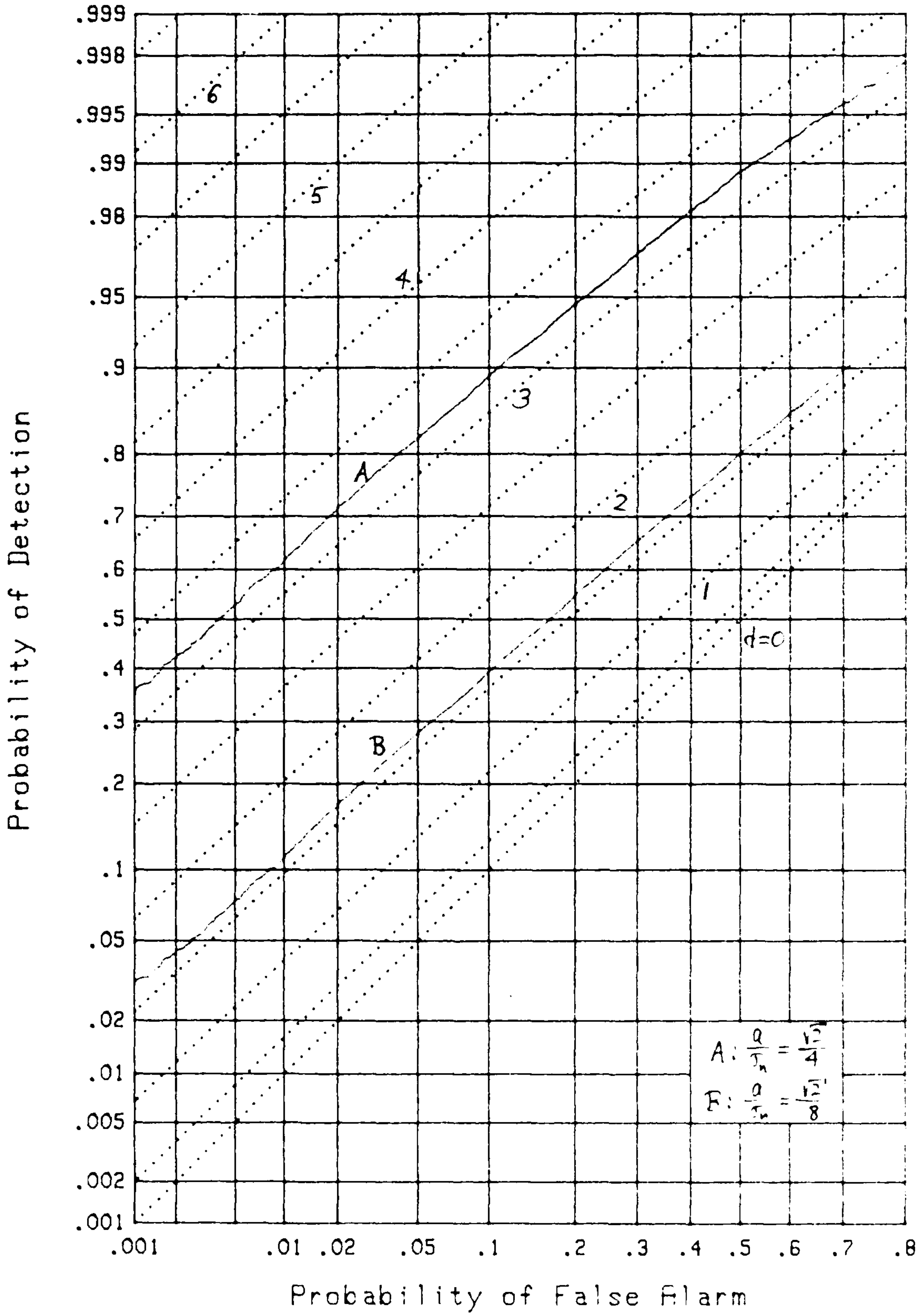

Figure 15. ROC for Narrowband, Clip Input, K=128

When K is decreased to 8, while a/σ_n is increased by a factor of 4, the same values result from the use of (93), as given in (97). The simulation results in figure 16 reveal that the actual performance of the narrowband correlator does not meet these deflection values 3.19 and 1.60, except at the upper right end of the curves. The reasons for the discrepancy are two-fold: K = 8 is not large enough to rely on the Gaussian approximation, and input signal-to-noise ratios, $a/\sigma_n = \sqrt{2}$ and $1/\sqrt{2}$, are not small, as assumed in (81) et seq.

When both the input and the reference are clipped, the simulation results for K = 128 are displayed in figure 17. The corresponding theory is furnished by (92) and (65), and yields the results for $\Delta_r^{(1)}$ already listed in (94). They become

$$\Delta_r^{(1)} = \begin{Bmatrix} 2.87 \text{ for } a/\sigma_n = \sqrt{2}/4 \\ 1.44 \text{ for } a/\sigma_n = \sqrt{2}/8 \end{Bmatrix} \text{ for } K = 128 \text{ ,} \tag{98}$$

and are in excellent agreement with the simulations in figure 17.

For the alternative situation with K = 8, the appropriate values follow from (94) as

$$\Delta_r^{(1)} = \begin{Bmatrix} 2.95 \text{ for } a/\sigma_n = \sqrt{2} \\ 1.47 \text{ for } a/\sigma_n = 1/\sqrt{2} \end{Bmatrix} \text{ for } K = 8 \text{ .} \tag{99}$$

These values furnish a good approximation to the simulation results in figure 18 at the upper right end, but are optimistic over the rest of the range. The reasons for the discrepancy are again that K is not large and the input signal-to-noise ratio, a/σ_n, is not small.

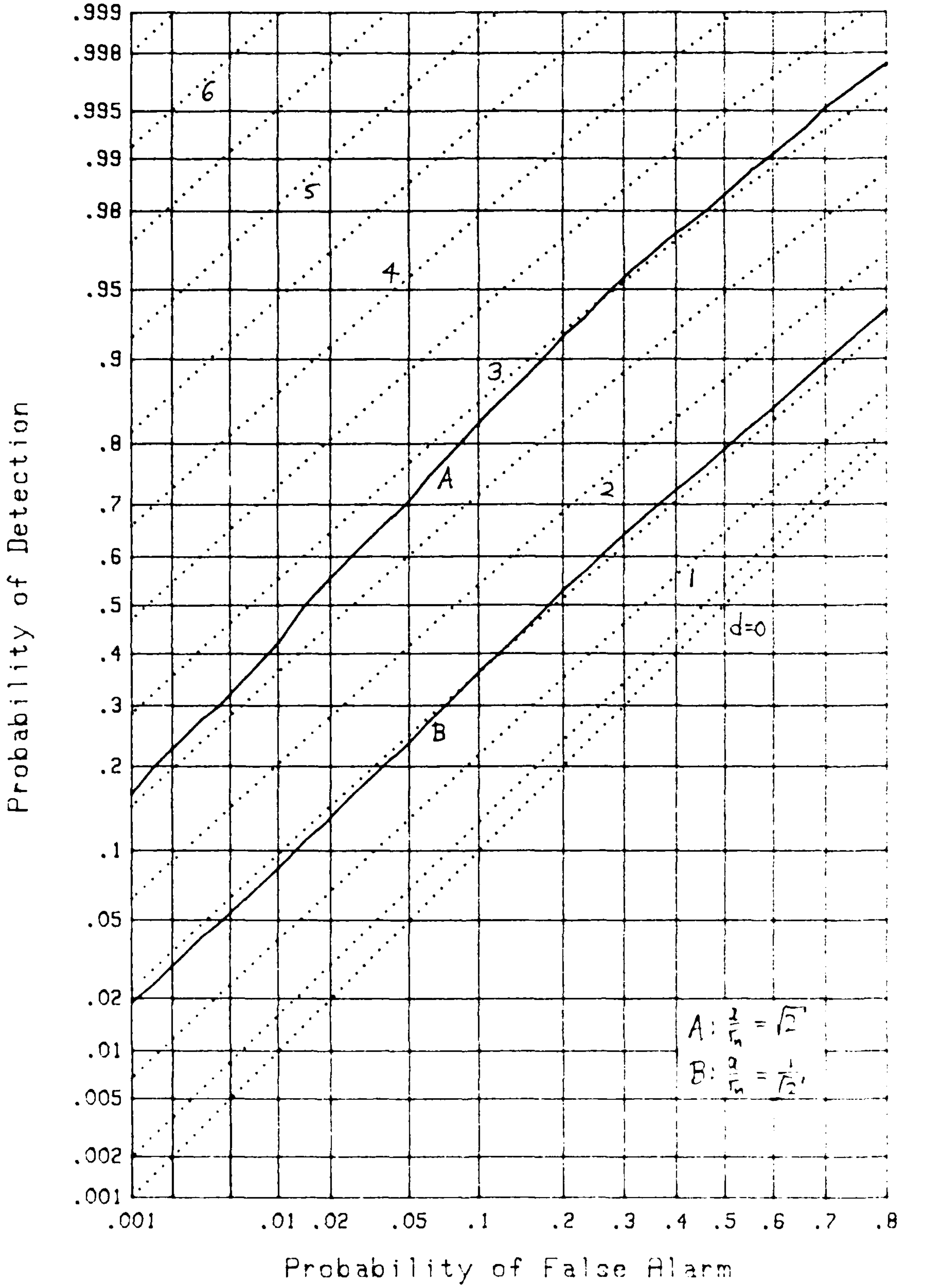

Figure 16. ROC for Narrowband, Clip Input, K=8

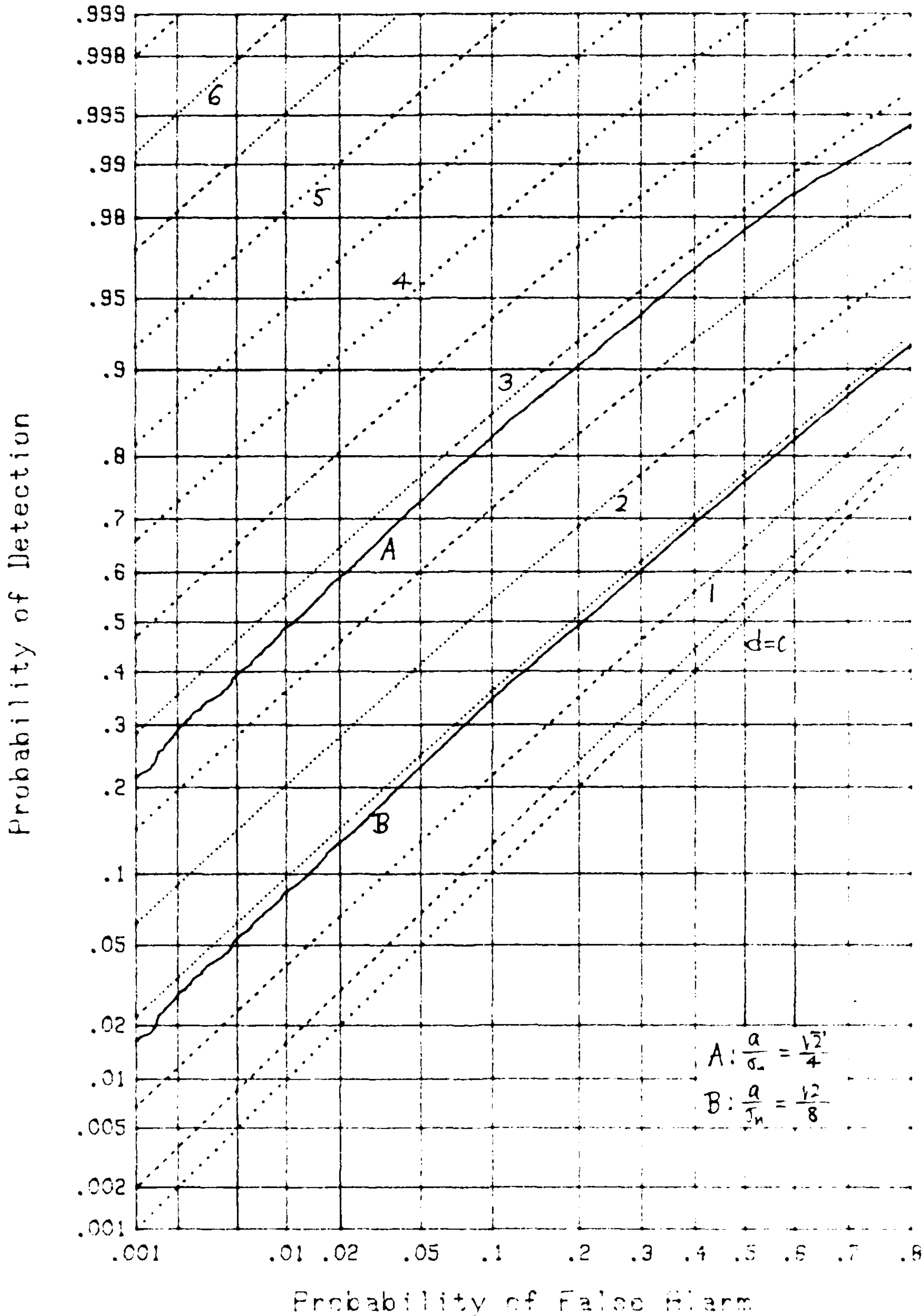

Figure 17. ROC for Narrowband, Clip Both, K=128

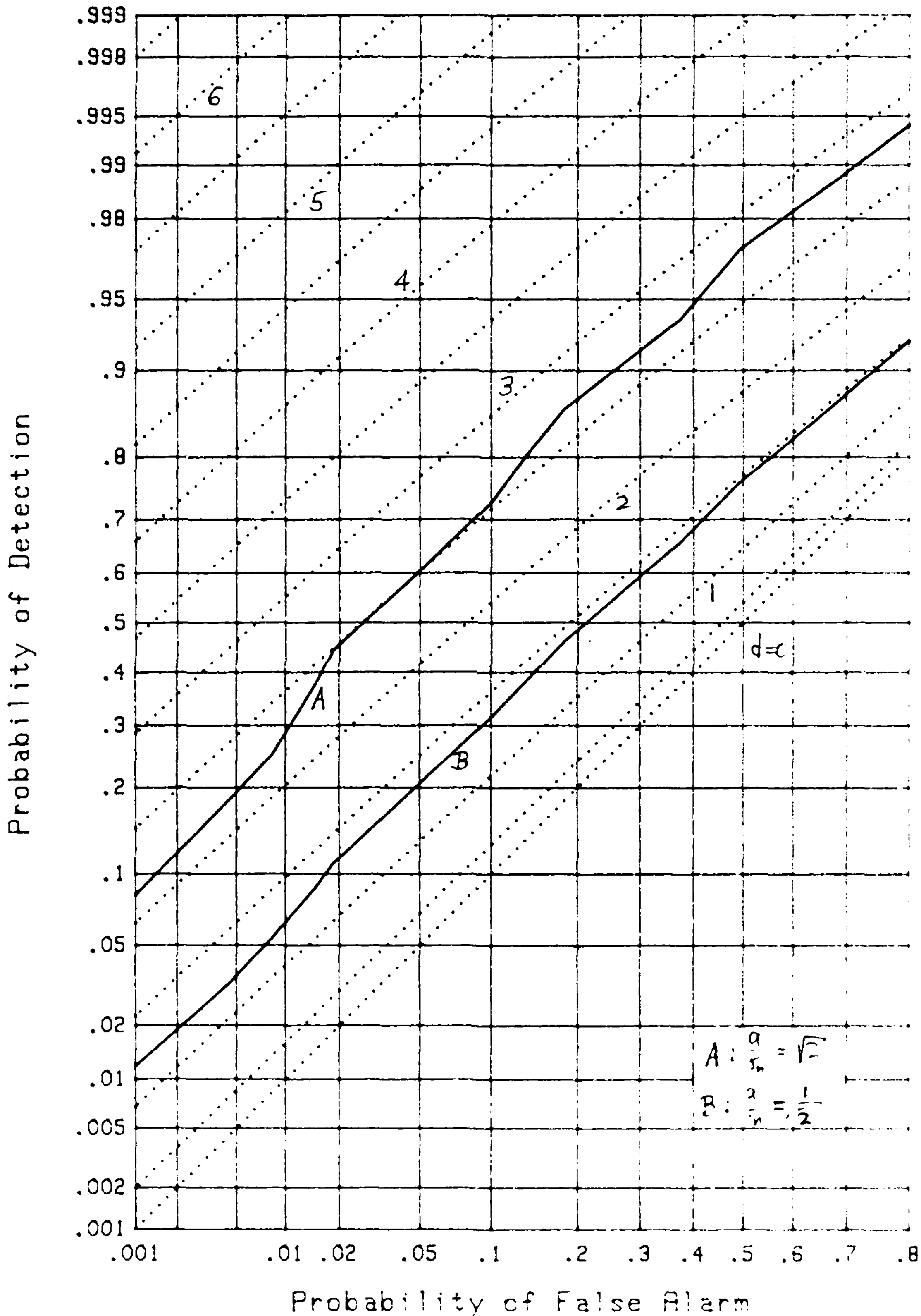

Figure 18. ROC for Narrowband, Clip Both, K=8

The final result in figure 19 is identical to the conditions of figure 17, except that now, the quadrature component of the clipped reference channels was suppressed; that is, only one real reference was used for multiplication in figure 10. The simulation results in figure 19 indicate $\Delta_r^{(1)}$ values of approximately 2.6 and 1.3; these values are approximately .9 dB poorer than (98) which pertained to figure 17. Thus, dropping one of the clipped reference channels causes a loss of almost 1 dB, and should be avoided.

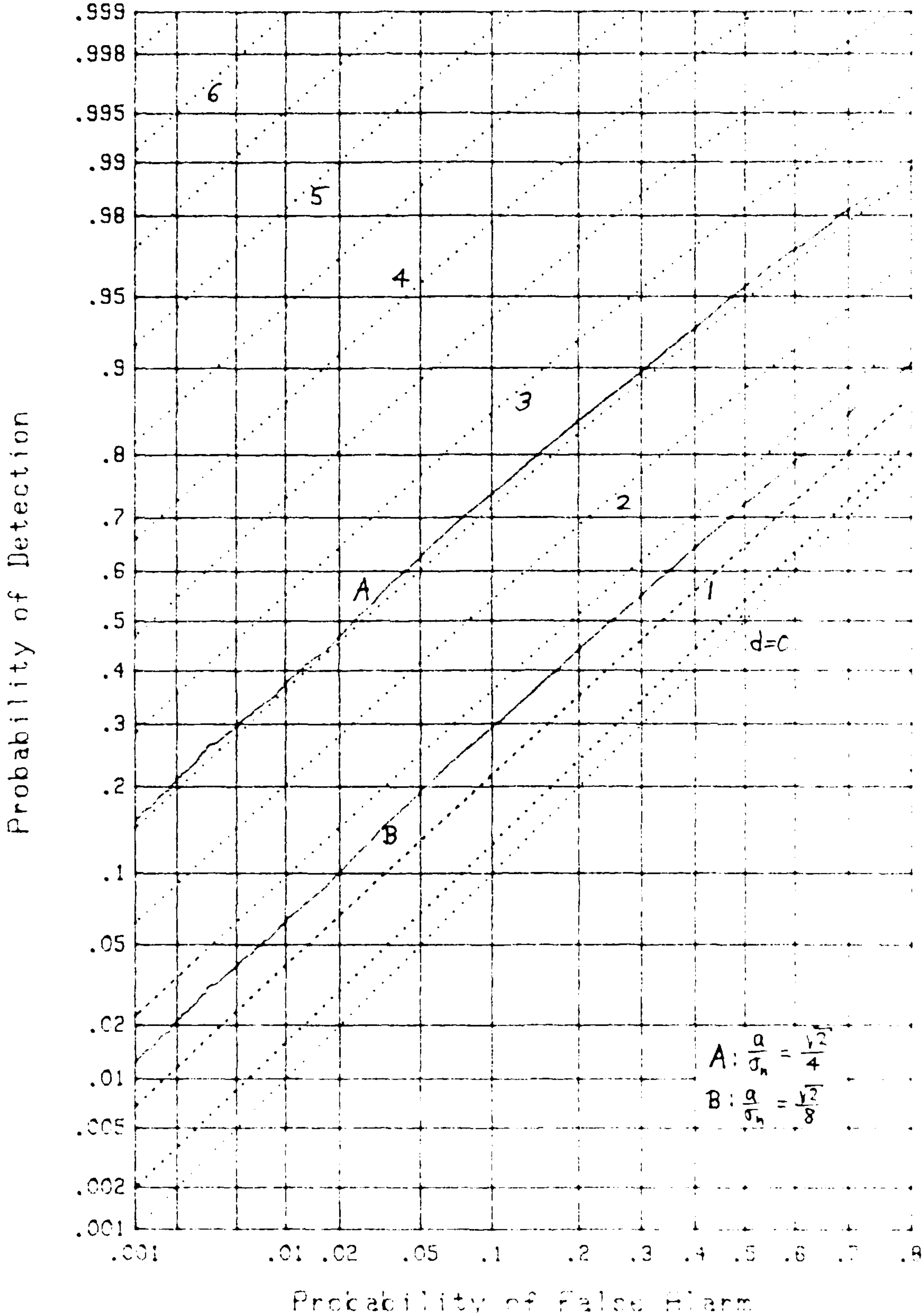

Figure 19. ROC for Narrowband, Clip One Reference, K=128

DISCUSSION/SUMMARY

Accurate prediction of performance of the baseband and narrowband correlators, with clipping at the input and/or reference levels, is possible over a wide range of number of input samples, input signal-to-noise ratio, and detection and false alarm probabilities. Only when K, the number of samples, gets too small to use the central limit theorem, does the theory begin to deviate from actual performance. However, it is precisely in this case that simulation is most attractive, since a large number of trials can then be conducted in a reasonable amount of time. Programs are furnished in the appendix, for both the baseband as well as the narrowband correlator, that enable extension of the simulation results to other cases of interest to the user.

If we compare corresponding results in the baseband and narrowband correlators, that is, figure 2 with figure 11, figure 3 with figure 12, etc., the predicted and simulation results for the deflections are identical, with one exception. Namely, when the reference is clipped and K is small, the narrowband deflections are slightly larger than the corresponding values for the baseband correlator; compare figure 5 with figure 14, and compare figure 9 with figure 18. Thus, the degradation suffered in the case of a narrowband correlator is not quite as bad as for the baseband correlator in these particular cases.

APPENDIX

PROGRAMS

The first program listed in this appendix pertains to the baseband correlator of figure 1, with both the input and reference clipped; see lines 320-350. If clipping is desired removed, merely delete SGN from the appropriate lines. This program is written in BASIC for the Hewlett-Packard 9000 computer; the qualifier DOUBLE in line 60 denotes INTEGER variables.

The second program pertains to the narrowband correlator depicted in figure 10, with both the input and reference clipped; see lines 370-400. If clipping is desired removed, delete the appropriate SGN operations.

```
10  ! CLIP INPUT AND REFERENCE; BASE BAND
20    I=30000                    !  NUMBER OF TRIALS
30    K=8                        !  NUMBER OF SAMPLES ADDED
40      As=2.                    !  INPUT SIGNAL AMPLITUDE a/σn
50      A$="BBB2"
60    DOUBLE I,K,Ks,Is           !  INTEGERS
70    DIM Z(1:30000),Cos(1:128)
80    REDIM Z(1:I),Cos(1:K)
90    R4=-LOG(4.)
100   T=2.*PI/K
110   FOR Ks=1 TO K
120   Phik=T*Ks
130   Cos(Ks)=COS(Phik)
140   NEXT Ks
150   FOR Is=1 TO I
160   Z=0.
170   FOR Ks=1 TO K-1 STEP 2
180   R1=RND-.5                  !  TWO
190   R2=RND-.5                  !  INDEPENDENT
200   R3=R1*R1+R2*R2             !  GAUSSIAN
210   IF R3>.25 THEN 180         !  RANDOM
220   R3=(R4-LOG(R3))/R3         !  VARIABLES
230   R3=SQR(R3+R3)              !  WITH ZERO
240   N1=R1*R3                   !  MEAN AND
250   N2=R2*R3                   !  UNIT VARIANCE
260   C1=Cos(Ks)
270   C2=Cos(Ks+1)
280   S1=As*C1
290   S2=As*C2
300   X1=S1+N1
310   X2=S2+N2
320   V1=SGN(X1)                 !  CLIP
330   V2=SGN(X2)                 !   INPUT
340   W1=SGN(C1)                 !  CLIP
350   W2=SGN(C2)                 !   REF
360   Z=Z+W1*V1+W2*V2
370   NEXT Ks
380   Z(Is)=Z
390   NEXT Is
400   MAT SORT Z(*)
410   Av=SUM(Z)/I
420   Var=DOT(Z,Z)/I-Av*Av
430   Sd=SQR(Var)
440   PRINT I;K;As;Av;Sd
450   MASS STORAGE IS ":C300,7"
460   CREATE DATA A$,1072
470   ASSIGN #1 TO A$
480   PRINT #1;Z(*)
490   ASSIGN #1 TO *
500   END
```

```
10   ! CLIP INPUT AND REFERENCE; NARROWBAND
20     I=30000                     !  NUMBER OF TRIALS
30     K=8                         !  NUMBER OF SAMPLES ADDED
40       As=SQR(2.)                !  INPUT SIGNAL AMPLITUDE a/σn
50       A$="BNB2"
60     DOUBLE I,K,Ks,Is            !  INTEGERS
70     DIM G2(1:30000),Cos(1:128),Sin(1:128)
80     REDIM G2(1:I),Cos(1:K),Sin(1:K)
90     R4=-LOG(4.)
100    T=2.*PI/K
110    FOR Ks=1 TO K
120    Phik=T*Ks
130    Cos(Ks)=COS(Phik)
140    Sin(Ks)=SIN(Phik)
150    NEXT Ks
160    T=2.*PI/I
170    FOR Is=1 TO I
180    Theta=T*Is
190    Ar=As*COS(Theta)
200    Ai=As*SIN(Theta)
210    Zr=Zi=0.
220    FOR Ks=1 TO K
230    R1=RND-.5                   !  TWO
240    R2=RND-.5                   !  INDEPENDENT
250    R3=R1*R1+R2*R2              !  GAUSSIAN
260    IF R3>.25 THEN 230          !  RANDOM
270    R3=(R4-LOG(R3))/R3          !  VARIABLES
280    R3=SQR(R3+R3)               !  WITH ZERO
290    Nr=R1*R3                    !  MEAN AND
300    Ni=R2*R3                    !  UNIT VARIANCE
310    Ck=Cos(Ks)
320    Sk=Sin(Ks)
330    Sr=Ar*Ck-Ai*Sk
340    Si=Ar*Sk+Ai*Ck
350    Xr=Sr+Nr
360    Xi=Si+Ni
370    Vr=SGN(Xr)                  !  CLIP
380    Vi=SGN(Xi)                  !   INPUT
390    Wr=SGN(Ck)                  !  CLIP
400    Wi=SGN(Sk)                  !   REF
410    Zr=Zr+Wr*Vr+Wi*Vi
420    Zi=Zi+Wr*Vi-Wi*Vr
430    NEXT Ks
440    G2(Is)=Zr*Zr+Zi*Zi
450    NEXT Is
460    MAT SORT G2(*)
470    Av=SUM(G2)/I
480    Var=DOT(G2,G2)/I-Av*Av
490    Sd=SQR(Var)
500    PRINT I;K;As;Av;Sd
510    MASS STORAGE IS ":CS80,7"
520    CREATE DATA A$,1072
530    ASSIGN #1 TO A$
540    PRINT #1;G2(*)
550    ASSIGN #1 TO *
560    END
```

REFERENCES

1. I. S. Gradshteyn and I. M. Ryzhik, Table of Integrals, Series, and Products, Academic Press, New York, 1965.

2. A. H. Nuttall, Some Integrals Involving the Q_M Function, NUSC Technical Report 4755, 15 May 1974.

INIITAL DISTRIBUTION LIST

Addressee	No. of Copies
ASN (RE&S)	1
OUSDR&E (Research and Advanced Technology)	2
DEPUTY USDR&E (Res & Adv Tech)	1
DEPUTY USDR&E (Dir Elect & Phys Sc)	1
ONR, ONR-100, -102, -200, -400, -410, 411 (N. Gerr), -422, -425AC, -430	9
COMSPAWARSYSCOM, SPAWAR 05 (W. R. Hunt)	2
CNO, OP-098, OP-941, OP-951	3
DIA (DT-2C)	10
NRL, Code 5132, (Dr. P. B. Abraham) Code 5370, (W. Gabriel), Code 5135, (N. Yen) (A. A. Gerlach)	4
USRD	1
NORDA	1
USOC, Code 240, Code 241	2
NAVSUBSUPACNLON	1
NAVOCEANO, Code 02	2
NAVELECSYSCOM, ELEX 03, 310	2
NAVSEASYSCOM, SEA-00, -05R, -06F, 63R (E. L. Plummer, CDR E. Graham IV, C. C. Walker), -92R	7
NAVAIRDEVCEN, Warminster	1
NAVAIRDEVCEN, Key West	1
NOSC, Code 8302, Code 6565 (Library), Code 713 (F. Harris)	3
NAVWPNSCEN	1
NCSC, Code 724	1
NAVCIVENGRLAB	1
NAVSWC	1
NAVSURFWPNCEN, Code U31	1
NISC,	1
CNET, Code 017	1
CNTT	1
NAVSUBSCOL	1
NAVTRAEQUIPCENT, Technical Library	1
NAVPGSCOL	2
NAVWARCOL	1
NETC	1
APL/UW, SEATTLE	1
ARL/PENN STATE, STATE COLLEGE	1
CENTER FOR NAVAL ANALYSES (ACQUISITION UNIT)	1
DTIC	2
DARPA, Alan Ellinthorpe	1
NOAA/ERL	1
NATIONAL RESEARCH COUNCIL	1
WOODS HOLE OCEANOGRAPHIC INSTITUTION (Dr. R. C. Spindel)	2
ENGINEERING SOCIETIES LIB, UNITED ENGRG CTR	1
NATIONAL INSTITUTE OF HEALTH	1
ARL, UNIV OF TEXAS	1

INIITAL DISTRIBUTION LIST

Addressee	No. of Copies
MARINE PHYSICAL LAB, SCRIPPS	1
UNIVERSITY OF CALIFORNIA, SAN DIEGO	1
NAVSURWEACTR	1
DELSI	1
DIRECTOR SACLANT ASW RES CEN	1
COM SPACE & NAV WAR SYS COM	1
COM NAVAL PERSONNEL R&D CENTER	1
COM NAV SUB COLLEGE	1
B-K DYN INC	1
BBN, Arlington, VA (Dr. H. Cox)	1
BBN, Cambridge, MA (H. Gish)	1
BBN, New London, CT (Dr. P. Cable)	1
EWASCTRI	1
MAR, INC, East Lyme, CT	1
HYDROINC (D. Clark)	1
SUMRESCR (M. Henry)	1
ANALTECHNS, N. Stonington, CT	1
ANALTECHNS, New London, CT	1
EDOCORP (J. Vincenzo)	1
TRA CORP., Austin, TX (Dr. T. Leih, J. Wilkinson)	2
TRA CORP., Groton, CT	1
NETS (R. Medeiros)	1
GESY, D. Bates	1
SONALYSIS, Waterford, CT (J. Morris)	1
ORI CO, INC. (G. Assard)	1
HUGHES AIRCRAFT CO. (S. Autrey)	1
MIT (Prof. A. Baggaroer)	1
RAYTHEON CO. (J. Bartram)	1
Dr. Julius Bendat, 833 Moraga Dr, Los Angeles, CA	1
COOLEY LABORATORY (Prof. T. Birdsall)	1
PROMETHEUS, INC. (Dr. James S. Byrnes)	1
BBN INC., New London, CT (Dr. P. Cable)	1
BBN INC., Arlington VA (Dr. H. Cox)	1
BBN INC., Cambridge, MA (H. Gish)	1
ROYAL MILITARY COLLEGE OF CANADA (Prof. Y. T. Chan)	1
UNIV. OF FLORIDA (D. C. Childers)	1
SANDIA NATIONAL LABORATORY (J. Claasen)	1
COGENT SYSTEMS, INC. (J. P. Costas)	1
IBM CORP. (G. Demuth)	1
UNIV. OF STRATHCLYDE, CLASGOW, SCOTLAND (Prof. T. Durrani)	1
ROCKWELL INTERNATIONAL CORP. (L. T. Einstein and Dr. D. F. Elliott)	2
GENERAL ELECTRIC CO. (Dr. M. Fitelson)	1
HONEYWELL, INC. (D. M. Goodfellow, Dr. Murray Simon, W. Hughey)	3
UNIV. OF TECHNOLOGY, LOUGHBOROUGH, LEICESTERSHIRE, ENGLAND (Prof. J. W. R. Griffiths)	1
HARRIS SCIENTIFIC SERVICES (B. Harris)	1

INITIAL DISTRIBUTION LIST

Addressee	No. of Copies
UNIV OF CALIFORNIA, SAN DIEGO (Prof. C. W. Helstrom)	1
EG&G (Dr. J. Hughen)	1
A&T, INC. (H. Jarvis)	1
BELL COMMUNICATIONS RESEARCH (J. F. Kaiser)	1
UNIV. OF RI (Prof. S. Kay, Prof. L. Scharf, Prof. D. Tufts)	3
MAGNAVOX GOV. & IND. ELEC. CO. (R. Kenefic)	1
DREXEL UNIV. (Prof. Stanislav Kesler)	1
UNIV. OF CT (Prof. C. H. Knapp)	1
APPLIED SEISMIC GROUP (R. Lacoss)	1
ADMIRALITY RESEARCH ESTABLISHMENT, ENGLAND (Dr. L. J. Lloyd)	1
NAVAL SYSTEMS DIV., SIMRAD SUBSEA A/S, NORWAY (E. B. Lunde)	1
DEFENCE RESEARCH ESTAB. ATLANTIC, DARTMOUTH, NOVA SCOTIA CANADA (B. E. Mackey, Library)	1
MARTIN MARIETTA AEROSPACE (S. L. Marple)	1
PSI MARINE SCIENCES (Dr. R. Mellen)	1
Dr. D. Middleton, 127 E. 91st St. NY, NY 10128	1
Dr. P. Mikhalevsky, 803 W. Broad St. Falls Church, VA 22046	1
CANBERRA COLLEGE OF ADV. EDUC., AUSTRALIA 2616 (P. Morgan)	1
NORTHEASTERN UNIV., (Prof. C. L. Nikias)	1
ASTRON RESEARCH & ENGR, (Dr. A. G. Piersol)	1
WESTINGHOUSE ELEC. CORP. (Dr. H. L. Price)	1
M/A-COM GOVT SYSTEMS, (Dr. R. Price)	1
DALHOUSIE UNIV. HALIFAX, NOVA SCOTIA (Dr. B. Ruddick)	1
NATO SACLANT ASW RESEARCH CENTER, LIBRARY, APO NY, NY 09019	1
YALE UNIV. (Prof. M. Schultheiss)	1
NATIONAL RADIO ASTRONOMY OBSERVATORY (F. Schwab)	1
DEFENSE SYSTEMS, INC (Dr. G. S. Sebestyen)	1
NATO SACLANT ASW RESEARCH CENTRE (Dr. E. J. Sullivan)	1
PENN STATE UNIV. APPLIED RESEARCH LAB. (F. W. Symons)	1
NAVAL PG SCHOOL, (Prof. C.W. Therrien)	1
DEFENCE RESEARCH ESTABLISHMENT PACIFIC, VICTORIA, B.C. CANADA VOS 1B0 (Dr. D. J. Thomson)	1
Robert J. Urick, 11701 Berwick Rd, Silver Spring, MD 20904	1
RCA CORP (H. Urkowitz)	1
USEA S.P.A. LA SPEZIA, ITALY (H. Van Asselt)	1
NORDA, Code 345 (R. Wagstaff)	1
TEL-AVIV UNIV. ISRAEL (Prof. E. Weinstein)	1
COAST GUARD ACADEMY (Prof. J. J. Wolcin)	1
SPACE PHYSICS LAB, UNIV OF ALBERTA, EDMONTON, CANADA (K. L. Yeung)	1
UNIV. OF IOWA (Prof. D. H. Youn)	1
COLOMBIA RESEARCH CORP. (W. Hahn)	1

END

12-87

DTIC